Forest response to increased disturbance in the Central Amazon and comparison to Western Amazonian forests

J. A. Holm[1], J. Q. Chambers[1,2], W. D. Collins[1,3], N. Higuchi[4]

[1] {Lawrence Berkeley National Laboratory, Berkeley, California 94720}

[2] {Department of Geography, University of California, Berkeley, Berkeley, California 94720}

[3] {Department of Earth and Planetary Science, University of California, Berkeley, Berkeley, California 94720}

[4] {Departamento de Silvicultura Tropical, Manejo Florestal, Instituto Nacional de Pesquisas da Amazônia, Av. André Araújo, 2936 Petrópolis, Manaus AM, Brasil}

Correspondence to: J. A. Holm (jaholm@lbl.gov)

Abstract

Uncertainties surrounding vegetation response to increased disturbance rates associated with climate change remains a major global change issue for Amazon forests. Additionally, turnover rates computed as the average of mortality and recruitment rates in the Western Amazon basin are doubled when compared to the Central Amazon, and notable gradients currently exist in specific wood density and aboveground biomass (AGB) between these two regions. This study investigates the extent to which the variation in disturbance regimes contributes to these regional gradients. To address this issue, we evaluated disturbance-recovery processes in a Central Amazon forest under two scenarios of increased disturbance rates using first ZELIG-TROP, a dynamic vegetation gap model which we calibrated using long-term inventory data, and second using the Community Land Model (CLM), a global land surface model that is part of the

Community Earth System Model (CESM). Upon doubling the mortality rate in the Central Amazon to mirror the natural disturbance regime in the Western Amazon of ~2% mortality, the two regions continued to differ in multiple forest processes. With the inclusion of elevated natural disturbances, at steady-state, AGB significantly decreased by 41.9% with no significant difference between modeled AGB and empirical AGB from the Western Amazon datasets (104 vs. 107 Mg C ha^{-1} respectively). However, different processes were responsible for the reductions in AGB between the models and empirical dataset. The empirical dataset suggests that a decrease in wood density is a driver leading to the reduction in AGB. While decreased stand basal area was the driver of AGB loss in ZELIG-TROP, a forest attribute that does not significantly vary across the Amazon Basin. Further comparisons found that stem density, specific wood density, and basal area growth rates differed between the two Amazonian regions. Last, to help quantify the impacts of increased disturbances on the climate and earth system, we evaluated the fidelity of tree mortality and disturbance in CLM. Similar to ZELIG-TROP, CLM predicted a net carbon loss of 49.9%, with an insignificant effect on aboveground net primary productivity (ANPP). Decreased leaf area index (LAI) was the driver of AGB loss in CLM, another forest attribute that does not significantly vary across the Amazon Basin, and the temporal variability in carbon stock and fluxes was not replicated in CLM. Our results suggest that: 1) the variability between regions cannot be entirely explained by the variability in disturbance regime, but rather potentially sensitive to intrinsic environmental factors; or 2) the models are not accurately simulating all tropical forest characteristics in response to increased disturbances.

Keywords: aboveground biomass, CLM, disturbance-recovery, growth rates, mortality, specific wood density, tropical rain forest, ZELIG-TROP.

1 Introduction

One of the largest uncertainties in future terrestrial sources of atmospheric carbon dioxide results from changes to forest disturbance and tree mortality rates, specifically in tropical forests (Cox et al., 2000; 2004; DeFries et al., 2002; Clark, 2007; Pan et al., 2011). There has been evidence that climate change and forest disturbance are linked such that a changing climate can influence the timing, duration, and intensity of disturbance regimes (Overpeck et al., 1990; Dale et al., 2001; Anderegg et al., 2013). In the tropics, climate change related impacts such as water and heat stress, and increased vulnerability to fires could lead to increased forest dieback (i.e., tree mortality notably higher than usual mortality) and increased disturbance rates (Cox et al., 2004; Malhi et al., 2008; 2009; U.S. DOE 2012). Increased forest dieback in tropical locations could then produce large economic costs, ecological impacts, and lead to climate related positive feedback cycles (Canham and Marks 1985; Dale et al., 2001; Laurance and Williamson 2001, Bonan 2008).

The effects of large-scale removal of tropical forest, leading to changes in global climate have been studied within global general circulation models (GCMs) (Shukla et al., 1990; Henderson-Sellers et al., 1993; Hahmann and Dickinson 1997; Gedney and Valdes 2000; Avissar and Werth 2005). For example, a rapid and complete deforestation of the diverse Amazon Basin was predicted to be irreversible (Shukla et al., 1990), losing ~180 Gt carbon. These past studies have simulated extreme deforestation, or complete removal of the tropical forest biome, with the goal of evaluating climate impacts (i.e., albedo, evaporation, precipitation, surface boundary conditions). However, instead of sudden and complete removal, gradual increases and spatially heterogeneous patterns of tropical tree mortality due to multiple causes are more likely to occur than complete loss (Fearnside 2005; Morton et al., 2006). In addition, the effectiveness of climate

70 mitigation strategies will be affected by future changes in natural disturbances regimes (IPCC
71 2014; Le Page et al., 2013), due to the effect of disturbances on the terrestrial carbon balance. By
72 using an economic/energy integrated assessment model, it was found that when natural
73 disturbance rates are doubled and in order to reach a stringent mitigation target, (3.7 W m^{-2} level)
74 the societal, technological, and economic strategies will be up to 2.5 times more costly (Le Page
75 et al., 2013). Due to the strong feedbacks from terrestrial processes, there is a need to utilize an
76 integrated Earth System Model approach (i.e., iESM; Jones et al., 2013) where an integrated
77 assessment model is coupled with a biogeochemical and biophysical climate model such as
78 CLM/CESM. It is necessary to improve earth system models in order to simulate dynamic
79 disturbance rates and gradual forest biomass loss in response to increasing mortality rates.
80 Turnover rates currently vary for different regions of Amazonia (Baker et al., 2004a;
81 2004b; Lewis et al., 2004; Phillips et al., 2004; Chao et al. 2009), with Central Amazon forests
82 having "slower" turnover rates, and the Western and Southern Amazon forests (which we call
83 'west and south') exhibiting "faster" turnover rates. This regional variation in turnover rates is
84 connected with differences in carbon stocks, growth rates, specific wood density, and
85 biodiversity. Baker et al. (2004a) investigated regional-scale AGB estimates, concluding that
86 differences in species composition and related specific wood density determined the regional
87 patterns in AGB. There is a strong west-east gradient in that 'west and south' Amazon forests
88 were found to have significantly lower AGB than their eastern counterparts; also confirmed by
89 additional studies (Malhi et al., 2006, Baraloto et al., 2011).
90 It is unclear if these regional variations in forest processes and carbon stocks are driven by
91 external disturbance (e.g., increased drought, windstorm, forest fragmentation) or internal
92 influences (e.g., soil quality, phosphorus limitation, species composition, wood density) (Phillips

et al., 2004; Chao et al. 2009; Quesada et al., 2010; Yang et al., 2013). Investigating the causes that drive variation in tree dynamics in the Amazon, in order to understand consequences for future carbon stocks for each region should still be explored. For example, are the differences in forest structure and function between the two regions a result of the disturbance regime? If the Central Amazon forests were subject to a higher disturbance regime and turnover rates similar to that of the 'west and south', would the two regions match in terms of forest dynamics, carbon stocks and fluxes? A goal of this paper is to use modeling tools to explore the influence of disturbance regimes on net carbon stocks and fluxes in the Central Amazon, and then compare to observational data from the 'west and south' regions of the Amazon.

We are using an individual-based, demographic, gap-model (Botkin et al., 1972; Shugart, 2002) as a "benchmark" model to 1) evaluate the influence of disturbance on net carbon loss and variations in forest dynamics between two regions (central vs. 'west and south'), 2) evaluate disturbance and mortality in CLM-CN 4.5 (called CLM for remainder of paper), and 3) improve upon representing terrestrial feedbacks more accurately in earth system modeling. We used the dynamic vegetation gap model ZELIG (Cumming and Burton 1993; Urban et al., 1993). ZELIG has been updated and modified to simulate a tropical forest in Puerto Rico with a new versatile disturbance routine (ZELIG-TROP; Holm et al., 2012), making this vegetation dynamic model a good choice for this study.

Vegetation and carbon response to increased disturbance rates resulting from human induced climate change must be examined in more detail. To test how a widely used global land surface model, CLM, forecasts changes in forest carbon sinks and sources we addressed differences in AGB, ANPP, growth rates, and coarse litter production rates as a result of disturbances. The main research questions of the study are: 1) what are the long-term

consequences of continual elevated disturbance rates and periodic, large-scale disturbances in the Central Amazon? 2) Can the variability in forest dynamics, carbon stocks and fluxes between the Western and Southern Amazon and the Central Amazon forests be explained by the variability in the natural disturbance regime (i.e., higher mortality rates)? Finally: 3) what are the differences after increasing disturbance rates in ZELIG-TROP vs. CLM for the Central Amazon? We are assuming an independent driver of mortality; therefore we are not assigning mortality to any particular cause. The final research question will evaluate the accuracy of CLM to predict changes to carbon fluxes due to increased disturbance, a process that is likely to increase with human induced climate change.

2 Methods

2.1 Study Area and Forest Inventory Plots

The empirical data used for this study were from two permanent transects inventoried from 1996-2006, located in reserves of the National Institute for Amazon Research (Instituto Nacional de Pequisas da Amazonia, INPA) in the Central Amazon in Brazil. The forest inventory transects are approximately 60 km north of Manaus, Brazil, in the Central Amazon where vegetation is old-growth closed-canopy tropical evergreen forest. The mean annual precipitation at Manaus was 2,110 mm yr^{-1} with a dry season from July – September, and mean annual temperature was 26.7°C (Chambers et al., 2004; National Oceanic and Atmospheric Administration, National Climatic Data Center, Asheville, N.C., USA). However, during 2003 to 2004, mean annual precipitation in the study area reached 2,739 mm yr^{-1}.

We quantified demographic data such as stem density, diameter at breast height (DBH, cm), and change in diameter for trees >10 cm DBH from census data from the two transects. This

139 data was used to calculate above-ground biomass (ABG) estimates (Mg C ha^{-1}) and were
140 determined using region-specific allometric equations after harvesting 315 trees in the Central
141 Amazon (Chambers et al., 2001; see eq. 1 below). This data was also used to estimate observed
142 values for above-ground net primary productivity (ANPP, Mg C ha^{-1} yr^{-1}) after taking into
143 account loss of tree mass due to tree damage (Chambers et al., 2001). Observed mortality rates (%
144 stems yr^{-1}) were based on census intervals ranging from 1 to 5 years on 21 1-ha undisturbed plots
145 located in the Biomass and Nutrient Experiment (BIONTE), and the Biological Dynamics and
146 Forest Fragments Project (BDFFP), also located in INPA (Chambers et al., 2004). We compared
147 model predictions from ZELIG-TROP to observed field data.
148 In order to test whether the variability in forest dynamics and carbon stocks between the
149 'west and south' and the Central Amazon forests can be explained by the variability in the natural
150 disturbance regime, we used forest inventory data collected and reported in Baker et al. (2004a)
151 and Phillips et al. (2004). We used inventory data collected from 59 plots as reported in Baker et
152 al. (2004a; 2004b), and from 97 plots as reported in Phillips et al. (2004) with these plots
153 constituting a large part of the RAINFOR Amazon forest inventory network (Malhi et al., 2002).
154 Sites occur across a large range of environmental gradients, such as varying soil types and level of
155 seasonal flooding, however all sites are considered to be mature tropical forests. We then
156 compared the Central Amazon forests (both simulated and observed data) to the observed 'west
157 and south' datasets.
158

159 **2.2 Description of ZELIG-TROP**

160 ZELIG-TROP is an individual based gap model developed to simulate tropical forests
161 (Holm et al., 2012). It is derived from the gap model ZELIG (Urban 1990; 2000; Urban et al.,

1991; 1993), which is based on the original principles of the JABOWA (Botkin et al. 1972) and FORET forest gap models (Shugart and West, 1977). ZELIG-TROP follows the regeneration, growth, development, and death of each individual tree within dynamic environmental conditions across many plots (400m^2 plots, replicated uniquely 100 times). Maximum potential tree behaviors (e.g. optimal tree establishment, diameter growth, and survival rates) are reduced as a function of light conditions, soil moisture, level of soil fertility resources, and temperature. Specific details on the ZELIG model modifications to create ZELIG-TROP can be found in Holm et al. (2012). Gap models have been used extensively to forecast forest change from varying types and levels of disturbances, such as windstorms and hurricanes (O'Brien et al., 1992; Mailly et al., 2000); simulate vegetation dynamics in response to global change (Solomon 1986; Smith and Urban 1988; Smith and Tirpak 1989; Overpeck et al., 1990; Shugart et al., 1992); and explore feedbacks between climate change and vegetation cover (Shuman et al., 2011; Lutz et al., 2013). ZELIG has been used to simulate forest succession dynamics in many forest types across the globe (O'Brien et al., 1992; Seagle and Liang 2001; Busing and Solomon 2004; Larocque et al., 2006; Nakayama 2008). (Descriptions of the plant mortality algorithm as well as definitions of terms and parameters used in ZELIG-TROP are provided in the supplemental material).

2.3 Model Parameterization for the Central Amazon

The silvicultural and biological parameters for each of the 90 tropical tree species required for ZELIG-TROP are found in Table 1. The 90 tree species consist of 25 different families, 54 canopy species, 18 emergent species, 12 sub-canopy species, and 6 pioneer species (Table 1). While these tree species do not represent all existing species found in the Central Amazon forest, they represent a diverse array of family types, canopy growth forms, and demographic traits such

185 as growth rates, stress tolerances, and recruitment variations that will produce a robust and
186 reliable result. The majority of the data used to parameterize ZELIG-TROP for the Amazon was
187 derived from a long-term (14-18 years) demographic study to estimate tree longevity (Laurance et
188 al., 2004) located in Central Amazon. Data was collected on 3159 individual trees from 24
189 permanent, 1 ha plots which span across an area of 1000 km^2 (Laurance et al., 2004). Wood
190 density data for the 90 species used in this study were gathered from published sources with sites
191 across South America (Fearnside, 1997; Chave et al., 2006).
192 We used results found by Laurance et al. (2004) to determine several parameters;
193 specifically the maximum age of the species (AGEMAX), the maximum diameter at breast height
194 (DBH_{max}, cm), and the growth-rate scaling coefficient (G) for ZELIG-TROP. AGEMAX was
195 found by taking the mean of three longevity estimates. DBH_{max} were scaled to match a more
196 accurate representation of maximum DBH in the simulated field sites (Chambers et al., 2004). We
197 used the canopy classification as described by Laurance et al. (2004) to infer species-specific
198 rankings for tolerance and intolerance to shading. Average monthly precipitation (cm) and
199 temperature (°C) required for the environmental parameters in ZELIG-TROP (Table 2) were
200 based on field data collected from 2002-2004 in the study site (Tribuzy, 2005). Soil field capacity
201 (cm) and soil wilting point (cm) were determined from soil measurements in nearby central
202 Amazon study sites (Laurance et al., 1999).
203 In order to more accurately simulate the Central Amazonian forest, a few modifications
204 were made to the original ZELIG-TROP model (Holm et al., 2012). First, the allometric equation
205 used to estimate above-ground biomass (Mg C ha^{-1}) was updated to include an equation specific
206 for the Brazilian rainforest in the Central Amazon (Chambers et al., 2001; Eq. 1).
207 $$\ln(mass) = \alpha + \beta_1 \ln(DBH) + \beta_2[\ln(DBH)]^2 + \beta_3[\ln(DBH)]^3 \quad (1)$$

where above-ground biomass (mass) is in kg, α is -0.370, β_1 is 0.333, β_2 is 0.933, and β_3 is -0.122 (r^2_{adj} = 0.973) based upon data collected from 315 harvested trees. Specific wood density is not taken into account in this model.

In model development of the original ZELIG-TROP (modified for a subtropical dry forest), death caused by natural mortality (age-related) was killing tropical trees prematurely. This was also seen in initial model testing for the wet tropical forest. In contrast to tropical dry forests, individuals in tropical wet forests have a longer life potential and a higher likelihood of reaching their potential size. For example, the Central Amazon is able to support trees >1000 years old (Chambers et al., 1998; 2001; Laurance et al., 2004), where a dry forest may only be able to support trees to a maximum of 400 years. To adjust for this variation, the natural survivorship rate was increased from 1.5% to 6% of trees surviving to their maximum age (Table 1). This was a conservative value, with one study estimating about 15% of species in Central Amazon attaining their maximum ages (Laurance et al., 2004). Lastly, we also modified ZELIG-TROP's mean available light growing factor algorithm, which in part was used to accurately calculate tree height and crown interaction effects, as developed in ZELIG-CFS (Larocque et al., 2011). To best portray tree growth and crown development typical of an individual within a tropical canopy, we used an earlier algorithm version developed for ZELIG-CFS. This algorithm was the ratio of available growing light factor (ALGF) to a doubled crown width for each individual, thereby adjusting the ALGF relative to horizontal space occupied by the crown and improving the predictive capacities of ZELIG-TROP for the Amazon. This modification thus affected the light extinction on tree growth, allowed more available light from the top to the bottom of the individual-tree crown, and in turn better predicted observed data of basal area growth and abundance of stems per plot.

231

232 ### 2.3.1 Verification Methods

233 ZELIG-TROP simulations for the Central Amazon forest were run for 500 years and
234 replicated on 100 independent plots, each the size of 400m^2. All simulations began from bare
235 ground, and results from ZELIG-TROP were averaged over the final 100 years of simulation.
236 This was the period when forest dynamics (e.g. stem density, AGB, ANPP) were seen to reach a
237 stable state and represent a mature forest stand. The model was verified by comparing the
238 following five simulated forest attributes (average ± SD) to observed field data from the two
239 inventory transects: (1) total basal area (m^2 ha^{-1}); (2) total AGB (Mg C ha^{-1}); (3) total stem density
240 (ha^{-1}); (4) leaf area index; and (5) ANPP (Mg C ha^{-1} yr^{-1}). To test model validity for the Central
241 Amazon forest we report percent difference between the observed and simulated results (Table 3).
242

243 ## 2.4 Disturbance Treatments

244 To better understand the long-term consequences of high disturbance in a Central Amazon
245 rainforest, we crafted a simulation that doubled annual background tree mortality in both ZELIG-
246 TROP and CLM assuming an independent mechanism as the driver of mortality. A description of
247 the Community Land Model (CLM) can be found in the supplementary materials. Predicting the
248 impacts of increased mortality is critical since other recent studies have found that tree mortality
249 in the Central Amazon has been undersampled in plot-based approaches, and after analyzing a
250 larger range of gap sizes (including larger gaps), ~9.1 to 16.9% of tree mortality was missing
251 (Chambers et al., 2013). The majority of gaps created in Amazonian rainforests are from
252 windthrow of canopy trees with a large percentage of gaps having relatively small areas of <200
253 m^2 (Uhl, 1982; Denslow, 1987; Stanford, 1990). However, some windthrow events will create

254 large gaps that then initiate secondary succession processes (Brokaw, 1985, Chambers et al.,
255 2013). Since there can be multiple spatial scales and drivers of tree mortality, we are simulating
256 mortality as a stochastic, independent event within ZELIG-TROP, using the new versatile
257 disturbance routine implemented in Holm et al. (2012). Most mortality events in the Central
258 Amazon occur on individual trees (Chambers et al., 2004; 2013). Therefore, this phenomenon was
259 replicated in the model. Specifically, any one tree >10cm DBH was randomly selected to die and
260 be removed from the forest canopy on an annual basis at the gap scale, in addition to the existing
261 selection of trees removed by natural senescence. This 'high disturbance' treatment for the
262 Central Amazon forests is representative of the current turnover rates in 'west and south' (Phillips
263 et al., 2004), thus creating an opportunity to test whether the variability in forest dynamics and
264 carbon stocks between the 'west and south' and the Central Amazon forests can be explained by
265 the variability in the natural disturbance regime. Variables compared between the two regions
266 included AGB, wood density (Baker et al., 2004a), recruitment rates, and stem density (Phillips et
267 al., 2004), and stand-level BA growth rates (Lewis et al., 2004).
268 A second treatment has been applied in order to improve understanding of periodic large-
269 scale disturbance and recovery events. This treatment consisted of removing 20% of stems >10cm
270 DBH every 50 years (i.e. periodic treatment). It has recently been noted that patch-scale ($400m^2$)
271 succession-inducing disturbances exhibit a return frequency of about 50 years within the Central
272 Amazon region (Chambers et al., 2013). Therefore we have set our large-scale disturbance event
273 to repeat four times over a 200 year period (every 50 years) after the forest has reached a mature
274 stable state. This treatment was also conducted in both ZELIG-TROP and CLM. An important
275 metric in determining the forest carbon balance as a result of disturbance is the total change in

stand biomass over time (ΔAGB, Mg C ha^{-1}), defined as $AGB_{t2} - AGB_{t1}$ over the simulation period.

3 Results

3.1 Model Verification Results

Results simulated by ZELIG-TROP for the mature Central Amazon tropical forest (pre-disturbance treatment) were in close range (e.g., within 17%) to empirical data (Table 3), making ZELIG-TROP successful at predicting stand dynamics of a complex tropical forest. Average basal area was 9.7% higher than the observed value (32.96 vs. 30.06 m^2 ha^{-1}), average AGB was 5.0% higher (178.38 vs. 169.84 Mg C ha^{-1}), and average leaf area index (LAI) was 1.8% higher (5.8 vs. 5.7). ZELIG-TROP predicted average stem density to be 12.5% lower (574 vs. 656 stems ha^{-1}), and ANPP was 17.1% lower than observed values reported by Chambers et al. (2001) (5.4 vs. 6.5 Mg C ha^{-1} yr^{-1}). ZELIG-TROP was also successful at accurately predicting stem density and AGB by DBH (cm) size class (Fig. 1a, 1c). The model over predicted the number of stems in the lowest size class (10-20 cm), by an additional 84 stems per hectare, and in the eighth size class (80-90 cm), but for the remaining size classes values were near to the observed data. Even with these slight over predictions in certain DBH size classes, the model predicted AGB to be within a reasonable range (8.5 Mg C ha^{-1}) of the observed values ($r^2 = 0.60$).

ZELIG-TROP was also able to predict a realistic community composition (Fig. 2a). After initiating the model from bare ground, there was a sudden increase in basal area per species, followed by a typical jigsaw pattern of die-offs and growth increases, with the model reaching a steady-state during the last 100 years. The dominant species in terms of basal area, (*Parkia multijuga*), a large, fast-growing emergent species from the Leguminosae family accounted for

299 17% of the total basal area in the last 100 years of simulation. The next four dominant species
300 were all canopy-level species. This was an accurate representation of the forest, as the canopy
301 layer consists of many tree crowns, large trees, and usually a dense area of biodiversity (Wirth et
302 al., 2001). For example, 63% of the 90 tree species simulated were categorized as a canopy
303 growth form. However, there was also an even mixture of emergent, sub-canopy, and pioneer
304 species as dominant and rare species, typical of a diverse Central Amazon forest. There was no
305 one single species that dominated the canopy throughout the course of the simulation. Instead, we
306 saw a diverse species representation (Fig. 2a). During the last 100 years of simulation, emergent
307 species represented 29.6% of the total basal area, sub-canopy species represented 1.7%, and
308 pioneer species represented 5.5% of the total basal area.
309 Empirical mortality rates (% stems yr^{-1}) from BDFFP and BIONTE data were log-
310 normally distributed averaging 1.02% ± 1.72% (Chambers et al. 2004). As estimated by ZELIG-
311 TROP, the no-disturbance annual mortality rates were near to observed values (1.27% ± 0.21%)
312 but had a smaller distribution around the mean (Fig. 3). As expected, annual mortality rate
313 doubled (2.66% ± 0.26%) for the high disturbance treatment.
314
315 **3.2 Central and Western Amazon Disturbance Comparisons**
316 **3.2.1 AGB, stem density, growth and recruitment rates**
317 Upon increasing the turnover rates of the Central Amazon forest to mirror the ~2% yr^{-1}
318 mortality rates in the 'west and south', the two Amazon regions continued to differ in forest
319 structure and function. Stem density, specific wood density, basal area growth rates, and AGB
320 from the treatment site did not match the trends observed in the 'west and south' plot network.
321 Using a Tukey's multiple comparison procedure following a one-way ANOVA, there was a

significant difference in both wood density and basal area growth rates between the two regions in the empirical dataset, but no significant difference in the model results (Fig. 4). Alternatively when comparing stem density there was no significant difference between the two regions in the empirical dataset, but there was a significant increase in the model results (Fig. 4).

The high disturbance treatment did significantly reduce AGB in the Central Amazon to values similar to the 'west and south' counterpart, but wood density was not included in the biomass allometric equation for the Central Amazon therefore this reduction in AGB was a 'false-positive'. Specifically, when the Central Amazon was subjected to faster turnover rates there was a significant reduction in AGB (two sample t-test, $t_{(99,1.97)} = 108.98$, $p<0.001$) and net carbon loss was 74 Mg C ha^{-1} (from 178 to 104 Mg C ha^{-1}) averaged over the last 100 years of simulation (Fig. 1d) equivalent to a 41.9% decrease. AGB in the Central Amazon was impacted the most by the high disturbance treatment. The AGB from the higher disturbed Central Amazon was similar (104 Mg C ha^{-1}) to AGB values in the 'west and south' RAINFOR network plots, but only when comparing to biomass equations that included weighting for wood density (Chave et al., 2001; Chambers et al., 2001). For example, AGB predicted by the Chave et al. (2001) equation (107 Mg C ha^{-1}), had no significant difference between the two disturbed regions (two sample t-test, $t_{(38, 2.7)} = 2.29$, considering alpha=0.01, p=0.03) (Fig. 4a). The significant reduction in stand basal area, and not variation in wood density, was the main driver of decrease in AGB in ZELIG-TROP (Fig. 5e). However, there was no significant difference in stand basal area between the empirical datasets in the Central and 'west and south' plots (p=0.368), a finding also confirmed by Baker et al. (2004a) and Malhi et al. (2006). While net carbon loss was the expected result, it constitutes a 'false positive' resulting from omitting wood density in the model estimate of biomass and from an absence of significant difference in stand basal area across the Amazonia field network.

345 The high disturbance treatment in the Central Amazon led to a significant increase in
346 stem density by 197 stems from 574 to 771 stems ha^{-1} (34.3% increase, Fig. 1b, two sample t-test,
347 $t_{(99,1.97)} = 28.06$, $p<0.001$). Compared to the regional gradient in the RAINFOR network there was
348 no significant difference between the higher disturbed and the Central Amazon empirical dataset
349 (573 stems ha^{-1} vs. 589 stems ha^{-1}) (two sample t-test, $t_{(46,2.01)} = 0.84$, $p=0.4077$, Fig. 4d). ANPP
350 did not significantly alter in the Central Amazon forest under a high disturbance treatment (two
351 sample t-test, $t_{(99,1.97)} = 1.54$, $p=0.1260$), only decreasing ANPP by 0.04 (from 5.39 to 5.35 Mg C
352 ha^{-1} yr^{-1}, 1.0%, Fig. 5a). Even with increased disturbance events, ANPP did not decrease in the
353 same manner as biomass due to recovery episodes from more frequent thinning and the increase
354 in smaller stems (i.e., 10 cm DBH size class) in newly opened gaps. When comparing the stand-
355 level BA growth rates (proxy for productivity) in the RAINFOR network there was a significant
356 increase in growth rates in the 'west and south' compared to the Central Amazon, but there was
357 no significant difference between the modeled treatments. In fact, an opposite response was seen,
358 and there was a slight decrease as a result of higher disturbance (by 0.21 m^2 ha^{-1} yr^{-1}, Fig. 4e or
359 0.20 Mg C ha^{-1} yr^{-1}, Fig. 5c). The model might be inaccurately representing growth rates because
360 prior to applying a higher disturbance regime in the Central Amazon, ZELIG-TROP significantly
361 over-estimated the stand-level growth compared to empirical data (3.2 vs. 1.4 m^2 ha^{-1} yr^{-1}).
362 The recruitment rates (% yr^{-1}) from the treatment site constitute the only variable that
363 matched the 'west and south' observational dataset. Under a high disturbance treatment in the
364 Central Amazon, as expected, there were subsequent increases in recruitment rate, where
365 recruitment significantly increased from 2.3 to 3.9% yr^{-1}, constituting a 69.1% increase above no-
366 disturbance recruitment rates (Table 4, Fig. 6a). Pre-treatment, modeled recruitment rates were
367 0.9% yr^{-1} higher compared to empirical values from the Central Amazon BDFFP plots (Phillips et

al., 2004). Recruitment and mortality rates are tightly linked (Lieberman et al., 1985), therefore when tree mortality increased, recruitment also significantly increased. In the 'west and south' empirical dataset recruitment rates were ~79% higher compared to the Central region (Fig. 4b). However, while turnover rates increased, there was *not* an increase in coarse litter production rate (trunks and large stems >10 cm diameter, Mg C ha^{-1} yr^{-1}, Fig. 6b) compared to the no-disturbance scenario, but rather a significant decrease (two sample t-test, $t_{(99,1.97)} = 2.70$, $p<0.01$). Under a high disturbance treatment, the production of coarse litter decreased by an average of 0.25 Mg C ha^{-1} yr^{-1} (8.3%, Table 4). However it is unclear if this decrease in production of coarse litter is biologically or atmospherically significant.

Once the forest reached a mature stable state (after 500 years) the periodic disturbance treatment was applied, removing 20% of stems in the mature forest every 50 years (for a duration of 200 years). The carbon loss over the 200-year period, including the four large-scale disturbances, was less severe than the high-disturbance treatment, but was still a significant decrease (two sample t-test, $t_{(99,1.97)} = 22.73$, $p<0.001$). Compared to the no-disturbance scenario, average AGB net carbon loss was 40 Mg C ha^{-1} (from 178 to 138 Mg C ha^{-1}, 22.7%, Fig. 7c) and ANPP significantly decreased from an average of 5.39 to 5.06 Mg C ha^{-1} yr^{-1} (6.1%, two sample t-test, $t_{(99,1.97)} = 7.65$, $p<0.001$). For the periodic treatment, the decrease in biomass was roughly half the decrease observed in the high-disturbance treatment, however the decrease in ANPP was more severe.

3.2.2 Community Composition Changes

The individual-based dynamic vegetation model approach was able to explore the long-term changes to community composition and fate of each species with increased disturbance. A

391 high disturbance treatment shifted species composition towards a more even canopy structure, and
392 increased the species evenness and diversity (Fig. 2b). The largest basal area reduction occurred
393 in the most common species; specifically the top two emergent species, followed by the most
394 common canopy species. With an increase in disturbance, the species originally occupying the
395 largest basal area on the plot, *Parkia multijuga*, decreased by 94.8% in relative difference in basal
396 area compared to all species averaged over the last 100 years. The next most common emergent
397 species, *Cariniana micrantha*, decreased by 32.6% with high disturbance, and canopy species
398 filled in as the dominant growth form (Fig. 2b).
399 The empirical dataset found wood density to be higher in the central region (~0.68 g cm^{-3}),
400 and lower in more disturbed 'west and south' (~0.57 g cm^{-3}) (Baker et al., 2004a). This trend was
401 not seen between the no-disturbance and high disturbance treatment in the central Amazon, with
402 no significant difference between the treatments (Fig. 4c). Before implementing the high
403 disturbance treatment average wood density was low for the non-disturbed Central Forest (0.59 g
404 cm^{-3}, similar to values of the 'west and south'), and with increased disturbances average wood
405 density increased (0.63 g cm^{-3}), an opposite response from empirical trends. Taking a closer look
406 at the community composition and representation of species, the emergent canopy class
407 experienced a decrease in basal area, amounting to 7.8% of total basal area, compared to 29.6%
408 prior to high disturbances. The three remaining growth forms all increased in basal area. The
409 emergent species had on average the highest wood density (0.72 g cm^{-3}), and the pioneer species
410 had on average the lowest wood density (0.52 g cm^{-3}). With a decrease in emergent species, it
411 would seem likely that average wood density would decrease, as expected in a forest with higher
412 turnover rates. However the dominant species prior to disturbance (the emergent: *Parkia*
413 *multijuga*), which experienced the largest decrease in basal area, had a very low wood density

414 (0.39 g cm^{-3}). In addition, even though the emergent size class decreased, the canopy species
415 (which also had high average wood density of 0.71 g cm^{-3}) basal area increased from 63% to
416 79.6%, and the increase in pioneer species from 5.5% to 5.9% was not sufficient to lower the total
417 wood density of the forest. With higher disturbance rates subcanopy species represented 6.7% of
418 the total basal area, compared to 1.7% prior to high disturbances.
419
420 **3.3 Disturbances and Carbon Change in CLM-CN 4.5 vs. ZELIG-TROP**
421 After applying a continual disturbance regime within CLM as in ZELIG-TROP, similar
422 patterns in forest biomass in response to disturbance were observed, and both models were in
423 agreement with each other. For example, the relative change in AGB was consistent (41.9% vs.
424 49.9% decrease) for ZELIG-TROP and CLM respectively (Fig. 5b). In CLM the aboveground
425 carbon storage pools are not determined using allometric equations, but rather through a carbon
426 allocation framework based off of photosynthesis, total GPP, and respiration (Thornton et al.,
427 2002). Including or excluding specific wood density is not considered in CLM. The model
428 outputs from CLM for the disturbed Central Amazon also showed a reduction in AGB similar to
429 the 'west and south'; which was also a 'false-positive' result. The significant loss of LAI with
430 disturbance was the main driver of reduction in AGB (Fig. 5f). There was a weak non-significant
431 difference in LAI between the empirical datasets in the Central and 'west and south' Amazon
432 regions ($p=0.077$). Another similarity between the two models was the non-significant change in
433 ANPP, however ZELIG-TROP predicted a decrease in ANPP while CLM predicted a slight
434 increase in ANPP (Fig. 5a).
435 With regards to the periodic disturbance treatment of large-scale disturbance events, CLM
436 also replicated analogous patterns in biomass loss and recovery as seen in ZELIG-TROP (Fig.

437 7c). In both models, the sudden decrease in biomass as well as re-equilibration during the
438 recovery phase matched. During each pulse disturbance, the forest lost on average 18.3% and
439 18.7% biomass in ZELIG-TROP and CLM respectively, and gained 16.5% and 15.4% biomass
440 during the recovery phase. Both CLM and ZELIG-TROP predicted that the recovering forest
441 biomass, on average, was less than the amount lost in each large-scale disturbance event,
442 therefore generating a negative total ΔAGB (-0.15 and -0.46 Mg C ha^{-1} yr^{-1} for ZELIG-TROP and
443 CLM respectively, Table 4). The negative total ΔAGB was less in ZELIG-TROP, and was likely
444 attributed to ZELIG-TROP predicting growth rates to significantly increase (by 0.20 Mg C ha^{-1}
445 yr^{-1}, two sample t-test, $t_{(99,1.97)} = 2.14$, $p<0.05$), most likely due to the open gaps from disturbance,
446 therefore losses were damped in ZELIG-TROP. In contrast CLM had growth rates that on average
447 decreased, due to the sharp decrease in growth rates following each large-scale disturbance event
448 (Fig. 7b). Both models also showed that each subsequent recovery period was always greater than
449 the previous period, up to a point where re-growth matched the biomass lost in the disturbance
450 event (Fig. 7c).
451 There were discrepancies with the response of ANPP to the periodic large-scale forest
452 mortality and recovery events between CLM and ZELIG-TROP. The immediate decrease in
453 ANPP following the large-scale disturbance event was significantly greater in CLM compared to
454 ZELIG-TROP (4.7 vs. 0.6 Mg C ha^{-1} yr^{-1}, Fig. 7a). The subsequent shape of ANPP during the 50-
455 year recovery was also different between the two models. CLM predicted that within
456 approximately two years after the disturbance, ANPP returned to pre-disturbance levels and
457 stayed relatively constant until the next disturbance. However, ZELIG-TROP did not display a
458 fast return to pre-disturbance levels, but instead predicted a gradual increase in ANPP after each
459 disturbance. Comparing the no-disturbance scenario and the periodic treatment, both models

460 predicted that overall ANPP significantly decreased with periodic disturbances (two sample t-test,
461 $p<0.001$ and $p=0.002$ for ZELIG-TROP and CLM respectively), however the gap model
462 predicted a greater percent difference in average ANPP; a 6.1% decrease vs. 3.5% decrease in
463 CLM.

464 To answer our last research question, what are the differences after increasing disturbance
465 rates in ZELIG-TROP vs. CLM for the Central Amazon, we did find other discrepancies. While
466 the magnitude of change between AGB was similar between the two models, CLM differs greatly
467 from ZELIG-TROP in that it did not captured the inter-annual variability in carbon stocks, while
468 ZELIG-TROP did (Fig. 5b). Therefore, the demographic forest model captured large fluctuations
469 in annual forest biomass and carbon stocks as a result of either gap dynamics, changes in
470 competition for resources, and/or varying size class and age class structure of the forest. In
471 addition, CLM did not produce pulses of coarse litter in response to tree mortality representative
472 of a heterogeneous landscape (Fig. 5d, 7d). While the relative change in AGB was consistent
473 between the two models, there was a large overestimation in the absolute values. With the
474 inclusion of the high disturbance treatment CLM predicted that average AGB net carbon loss was
475 134 Mg C ha^{-1} (from 269 to 135 Mg C ha^{-1}) vs. 74 Mg C ha^{-1} in ZELIG-TROP.
476

477 ## 4 Discussion

478 ### 4.1 Elevated forest disturbance and long-term impacts

479 Disturbance is likely to increase in Amazon forests. Since the mid-1970's observed tree
480 mortality and recruitment rates have been increasing in the Amazon (Phillips et al., 2004), and
481 higher than usual mortality rates have also been associated with droughts and strong windstorm
482 events (Nepstad et al., 2007; Chambers et al., 2009; Phillips et al, 2009; Negron-Juarez et al.,

483 2010; Lewis et al., 2011), each of which could increase with human-induced climate change. In
484 addition, reported mortality rates might be underestimated as 9.1-16.9% of tree mortality was
485 missing from plot-based estimates in the Amazon (Chambers et al., 2013). We first investigated
486 the impact of continual high disturbance (100 years) in a Central Amazonian forest using a
487 demographic forest model as a benchmark model due to operating at finer scales and having
488 mechanistic mortality algorithms. The elevated disturbance resulted in a decrease in AGB by
489 41.9%, with essentially no change in ANPP (1.0% decrease), and an increase in recruitment rates
490 by 69.1%. As a result of higher proportion of smaller stems (20.7% increase in the 10-30cm DBH
491 size classes), and decrease in large stems, there was a significant decrease in coarse litter
492 production rate by 8.3%.
493 We compared empirical data from the higher disturbed 'west and south' Amazon plots
494 ('fast dynamics'), to the modeled Central Amazon forest with mirrored tree mortality to evaluate
495 if the models used in this study could predict similar forest dynamics and characteristics. Only
496 one attribute that is tightly linked with disturbances (i.e., increase in recruitment) followed the
497 same pattern when shifting from low disturbance to high disturbance. The models were not
498 successful in predicting the shift in growth rates and specific wood density; forest processes and
499 traits that have been shown to differ with varying turnover rates (Baker et al., 2004a; Lewis et al.,
500 2004; Phillips et al., 2004). Therefore, results showed that the disturbance regime alone might not
501 explain all of the differences in forest dynamics between the two regions, or the models do not
502 accurately capture all disturbance and recovery processes. Furthermore, the net loss in biomass
503 was assumed to be a 'false-positive' in the models because in ZELIG-TROP AGB loss was driven
504 by basal area loss, and in CLM AGB loss was driven by LAI loss. Basal area and LAI are not
505 found to be drivers of AGB loss, or patterns of biomass, in empirical datasets (Baker et al., 2004a;

506 Malhi et al., 2006). In contrast basal area varied only slightly across the Amazon plot network
507 (27.5 vs. 29.9 m^2 ha^{-1}, Baker et al., 2004a). This indicates that wood density, which is a strong
508 indicator of functional traits (Whitmore, 1998); along with patterns of family composition are
509 strong drivers in steady-state AGB variation.

510 One study using the RAINFOR network found that variation in wood density drives the
511 pattern in regional-scale AGB (Baker et al., 2004a), a trend that was not captured in ZELIG-
512 TROP. While wood density is typically found to be higher in the central Amazon and lower in the
513 'west and south' (Baker et al., 2004a; ter Steege et al., 2006; Saatchi et al., 2009), high wood
514 density is also found in northern Peru (Patino et al., 2009; Saatchi et al., 2009). Next we
515 compared the same disturbance scenario in CLM-CN 4.5 and found with regards to AGB
516 response to disturbance, CLM performed in a very similar behavior to the gap model. CLM did
517 not reproduce the temporal variability in coarse litter inputs, and instead remained constant over
518 time. We also compared the response of large-scale periodic disturbances in the two models, and
519 found that CLM captured similar disturbance and recovery patterns as the gap model.

520 After applying continual and periodic higher disturbance treatments, we did not observe a
521 continual decrease in forest structure or biomass that lead to a new forest successional trajectory.
522 Instead, we found that the Amazon forest shifted to a new equilibrium state. The outcome of a
523 continual higher disturbance rate generated a stable forest but with less biomass, faster turnover,
524 higher stem density consisting of smaller stems, as well as less emergent species, less ANPP, and
525 less contribution of coarse litter inputs. Inventory studies have reported that with increased
526 turnover, there is a change in community composition, less wood density, and when these traits
527 are taken into account there is also less AGB (Baker et al., 2004a). We conclude that including
528 wood density in dynamic vegetation models is needed. While we have shown that terrestrial

biomass will decrease with increased disturbances, the interacting affects from potential CO_2 fertilization should be explored.

4.1.1 Disturbance, biomass accumulation, and CO_2 fertilization

Demographic vegetation models are useful tools at predicting long-term temporal trends related to changes in carbon stocks and fluxes. The offsetting interactions between possible CO_2 fertilization and disturbances are an important next step to evaluate. Based on observational studies from permanent plots there has been an increase in tree biomass in Amazonian forests by ~0.4-0.5 t C yr^{-1} over the past three decades (Lewis et al., 2004; Phillips et al., 1998; 2008). CO_2 fertilization effects might be an explanation (Fan et al., 1998; Norby et al., 2005), but this is unknown or refuted (Canadell et al., 2007, Norby et al. 2010), and manipulation experiments of enhanced CO_2 in the tropics is untested (Zhou et al., 2013). Due to the magnitude of forest growth, CO_2 fertilization may not be a causal factor but instead driven by interacting agents such as biogeography and changing environmental site conditions (Lewis et al., 2004; Malhi and Phillips, 2004). The role of widespread recovery from past disturbances still needs to be explored as an explanation for biomass accumulation.

In a study evaluating the risk of Amazonian forest dieback, Rammig et al. (2010) used rainfall projections from 24 GCMs and a dynamic vegetation model (LPJmL) and predicted that Amazon forest biomass is increasing due to strong CO_2 fertilization effects (3.9 to 6.2 kg C m^{-2}), and out ways the biomass loss due to projected precipitation changes, however larger uncertainties are associated with the effect of CO_2 compared to uncertainties in precipitation. Increasing evidence from an ensemble of updated global climate models are predicting that tropical forests are at a lower risk of forest dieback under climate change, in that they can still

552 retain carbon stocks until 2100 due to fertilization effects of CO_2 (Cox et al., 2013; Huntingford et
553 al., 2013), however there is still large uncertainties between models and how tropical forests will
554 respond to interacting effects of increasing CO_2 concentrations, warming temperatures, and
555 changing rainfall patterns (Cox et al., 2013).

556 In this study over the period of 100 years there was no significant change in biomass
557 accumulation in both ZELIG-TROP and CLM (Fig. 5b), and the forest did not act as a carbon
558 sink as predicted by empirical studies across a network of Amazon inventory plots (Phillips et al.,
559 1998; 2004). One explanation could be due to atmospheric CO_2 being held constant. Upon
560 applying the disturbance treatment, the forest became more stable. With regards to periodic
561 disturbances and sudden tree mortality events both models predicted a negative ΔAGB, -0.15 and
562 -0.46 Mg C ha^{-1} yr^{-1} for ZELIG-TROP and CLM respectively, therefore the forest acting as a
563 carbon source (Table 4). CLM predicted a larger decrease in biomass under periodic disturbances,
564 which offsets the current observed biomass accumulation (lower empirical estimates at 0.20-0.39
565 Mg C ha^{-1} yr^{-1} (Phillips et al., 1998; Chambers and Silver, 2004)).
566

567 ## 4.2 Lessons Learned from Modeling Tropical Forest Disturbance

568 ### 4.2.1 Model comparison to field data and additional sites

569 We found that using a dynamic vegetation gap model that operates at the species level was
570 successful at replicating the Central Amazon forest. ZELIG-TROP has also been validated for the
571 subtropical dry forest of Puerto Rico (Holm et al., 2012), but this is the first application of a
572 dynamic vegetation model of this kind (i.e., gap model) for the Amazon Basin. As a result of
573 using species-specific traits, the values reported by ZELIG-TROP for average basal area, AGB,
574 stem density, LAI, and ANPP were all close to observed values (e.g., ranging from 1.7 to 17.1 %

575 difference between ZELIG-TROP and observed field results). Field measurements of AGB from
576 the Central Amazon transects averaged ± SD: 169 ± 27.6 Mg C ha^{-1}, and additional field-based
577 measurements from nearby sites in the Central Amazon (FLONA Tapajós plots) range from 132
578 to 197 Mg C ha^{-1} (Miller et al., 2003; Keller et al., 2001). ZELIG-TROP predicted very similar
579 estimates of AGB: 178 ± 10.5 Mg C ha^{-1}, therefore model results were within the expected range.
580 From a single-point grid cell, located in the same latitude and longitude coordinates as
581 observational plots, CLM predicted higher levels of AGB (269 Mg C ha^{-1}). In a study comparable
582 to ours, Chambers et al. (2004) found that upon doubling turnover rates in an individual based
583 stand model, forest biomass for a Central Amazon forest decreased by slightly more than 50%.
584 This decrease in forest biomass was similar to the response reported in this study (41.9% and
585 49.9%). Unlike the Chambers et al. (2004) study, we did not impose an increase in growth rates in
586 the model parameters in conjunction with elevated turnover rates. Instead, annual growth rates
587 were determined internally within ZELIG-TROP based on species-specific parameters and
588 environmental conditions.
589

590 **4.2.2 Growth rates and wood density**

591 Our prediction of average growth rate was higher than field data found in the Central
592 Amazon BDFFP inventory plots (3.1 vs. 1.7 Mg C ha^{-1} yr^{-1}, Table 4), but similar to other values
593 found in the Central and Eastern Amazon. For example, using a process-based model, Hirsch et
594 al. (2004) found above-ground stem growth to be 3.6 Mg C ha^{-1} yr^{-1}, and field measurements were
595 2.9 Mg C ha^{-1} yr^{-1} at the Seca Floresta site in the Tapajós National Forest (Rice et al., 2004).
596 During the high disturbance treatment, we did not observe an increase in average growth rates
597 compared to the no-disturbance treatment. In fact, there was a slight decrease in annual growth

598 (Table 4, Fig. 4e). This non-significant change in growth rates could have been due to the
599 nonoccurrence of large increases in available light and resources after each additional death, a
600 result of a continual disturbance treatment as opposed to a dramatic disturbance event.
601 Alternatively the Western Amazon plots, counterparts to the high disturbance treatment, did
602 exhibit an increase in growth rates (Fig. 4e). Differences in environmental gradients between
603 regions, such as higher total phosphorous, less weathered, and more fertile soils in the Western
604 Amazon (Quesada et al., 2010) could be a stronger controlling factor. In the periodic disturbance
605 treatment, growth and productivity *did* increase directly following each large-scale disturbance
606 (i.e., removing 20% of stems). After each pulse disturbance ANPP increased by 14% over the 50-
607 year recovery phase. The change in community composition under the high disturbance treatment
608 was also representative of what would be expected (i.e. emergent species decreased by the largest
609 percent in basal area, and canopy and subcanopy species increased), however by not capturing
610 expected changes in wood density the model might be missing some shifts in species composition
611 response to disturbance.
612 Wood density is a robust indicator of life history strategies, growth rates, and/or
613 successional status of a forest (Whitmore, 1998; Suzuki, 1999; Baker et al., 2004a). Upon
614 modeling a Central Amazon forest with disturbance rates similar to the 'west and south', the
615 higher disturbance did *not* create a community composition dominated by pioneer species or
616 lower the average wood density, but instead created a forest of less emergent species, more
617 canopy species, and higher wood density. Our results further confirm that environmental and/or
618 stand factors explain the regional variation of AGB and wood density. Even with elevated
619 disturbance in the central Amazon the species that persisted and increased in basal area had on
620 average high wood density (0.7 g cm^{-3}). The growth rate scaling coefficients, G, used in ZELIG-

621 TROP were inversely correlated with wood density, matching the robust signal observed from
622 inventory data, but was not correlated (R^2=0.13), leading to a possible explanation of the opposite
623 pattern in wood density shifts with increased disturbance. Wood density is not a main
624 parameterization variable in ZELIG-TROP, and other factors in the gap model (e.g., drought or
625 light tolerances, maximum age, availability of light) could be a stronger driver of community
626 composition shifts over wood density.
627 It should be noted that wood density is difficult to measure accurately in the field, varies
628 between and within species (Chave et al., 2006), varies within a tree across diameter and from the
629 base of the tree to the top (Nogueira et al., 2005), and the Chambers et al. (2001) AGB model
630 without wood density shows that variation of the data explained by the model is strong (r^2 =
631 0.973). Including wood density in AGB allometric equations is not required, but beneficial for
632 accounting for differences in carbon stocks due to changes in species composition, gradients in
633 soil fertility (Muller-Landau, 2004) as opposed to disturbance regimes, and can be a key variable
634 in greenhouse gas emission mitigation programs.
635
636 **4.2.3 CLM 4.5 vs. dynamic vegetation model**
637 Simulating vegetation demography is beneficial to tracking community shifts, plant
638 competition, and dynamic changes in carbon stocks and fluxes, and should be considered being
639 incorporated into CLM. The version of CLM used here does not take into account differences
640 between plant size, plant age, or all biotic and abiotic stressors. Using demography typical of a
641 gap model will account for these missing factors, will aid in capturing annual carbon variability as
642 a result of heterogeneous mortality across the landscape, and can help improve global land surface
643 models. The exact causes and processes leading to plant mortality are difficult to quantify

644 (Franklin et al., 1987; McDowell et al., 2008; 2011), and additional field research is required in
645 this area, especially in the tropics. However, the gap model approach can quantify the
646 contribution due to natural death, stress related death, or disturbance related death under no-
647 disturbance and high-disturbance scenarios.

648 The major differences between the gap model ZELIG-TROP and CLM in response to
649 higher disturbance rates was, 1) the average AGB net carbon loss was 74 Mg C ha^{-1} in ZELIG-
650 TROP versus 134 Mg C ha^{-1} in CLM as a result of doubling background mortality, and 2) the
651 temporal variability in carbon stock and fluxes was not replicated in CLM. While the absolute
652 values in AGB net carbon loss were different between the two models (Fig. 5b), this was due to
653 the fact that ZELIG-TROP was calibrated for a specific location in the Central Amazon and CLM
654 using initial conditions representative of the entire Amazon basin. As a result of this distinction,
655 relative differences should be used as a comparison tool. The two models were consistent in that
656 they both reached new equilibrium steady-states with both continual and periodic disturbances,
657 and therefore the relative change in biomass was analogous between ZELIG-TROP and CLM.
658 Temporal variability in carbon stocks and fluxes over time were also absent from the CLM model
659 due to the inexistence of plant demography (i.e., changes in plant size, structure, and age).
660 Regarding the response to periodic disturbances, the major difference between ZELIG-TROP and
661 CLM was the rapid return to pre-disturbance ANPP levels in CLM after each large-scale
662 disturbance event, while in ZELIG-TROP the recovery of ANPP was gradual.

663 With the inclusion of higher disturbance rates, the two models tested here do predict a
664 ~40-50% reduction in carbon stocks, however the drivers that lead to biomass reduction are
665 inconsistent with the empirical driver. Additionally, ZELIG-TROP predicted lower coarse litter
666 production rates, and gains that exceeded losses. CLM predicted higher coarse litter production

667 rates, and losses that exceeded gains (Table 4), but these differences were minimal. However,
668 these differences that we found in gains minus losses between ZELIG-TROP and CLM can lead
669 to inaccurate predictions of carbon response to increasing disturbance rates in integrated
670 assessment models that use CLM. When taking into account the entire Amazon Basin over many
671 years, this discrepancy can significantly affect predictive outcomes when using the global CLM
672 for mitigation strategies.
673

674 ### 4.3 Future Directions and Summary

675 To constrain the future concentration of CO_2 into the atmosphere, current mitigation
676 strategies rely heavily on tropical forests to maintain, or increase, as a carbon sink. In order to
677 accurately develop and impose mitigation strategy targets, the land components of earth system
678 models need to more accurately simulate plant mortality, coarse litter inputs, carbon fluxes, and
679 accelerated growth processes associated with disturbance-recovery events. CLM 4.5 has been the
680 model of focus here, however multiple versions of the Lund-Potsdam-Jena Dynamic Global
681 Vegetation Model (LPJ-DGVM; Sitch et al., 2003), such as LPJ-GUESS (Smith et al., 2001),
682 LPJmL (Bondeau et al. 2007), and LPJ-SPITFIRE (Thonicke et al., 2010) are notable dynamic
683 vegetation models to evaluate changes to forest biomass in the Amazon (Rammig et al., 2010),
684 and changes to stand structure, plant mortality, and emissions due to fire (Thonicke et al., 2010).
685 Cramer et al. (2001) showed the varying range and uncertainties in ecosystem response and
686 magnitude of the terrestrial carbon sink as a function of rising CO_2 and climate change using six
687 DGVMs with varying degrees of functionalities. Including transient changes in vegetation
688 structure while accounting for changes due to elevated disturbance rates requires models to
689 include vegetation dynamics, succession processes, and biogeochemical processes. With the

690 varying degree of capabilities and functionality within vegetation models this study has
691 benchmarked mortality and disturbance processes in CLM and will benefit the iESM project
692 (Integrated Earth System Model; Jones et al., 2013), which combines CLM with a fully integrated
693 human system component. The capability of tropical forests to act as a carbon sink with and
694 without the inclusion of disturbances needs to be corrected in some models. If not, incorrect
695 predictions of the land uptake could either diminish the effect of mitigation policy, or force more
696 stringent changes in energy infrastructure in order to meet the same climate stabilization targets.
697 Ultimately the contributions to iESM will create the capabilities to test the carbon market and
698 energy market responses to changes in forest mortality and increased disturbances in the Amazon
699 and on a global scale.

700 It is predicted that disturbances will increase in the future, and this modeling study was
701 unique in that we: 1) showed that the drivers that lead to the net loss in carbon stocks in two
702 models are different compared to drivers in empirical datasets, 2) predicted that not all differences
703 in tropical forest attributes (e.g., AGB, basal area growth, stem density, and wood density) can be
704 explained by the disturbance regime alone, and also 3) highlighted some inconsistencies between
705 a detailed gap model and the global community land surface model used in CESM. It was also
706 unique in that we simulated a *continual* high disturbance rate, in addition to background mortality
707 during each time step. This set it apart from the majority of disturbance studies that have
708 simulated a one-time total deforestation of the Amazon (Shukla et al., 1990; Henderson-Sellers et
709 al., 1993; Hahmann and Dickinson, 1997; Gedney and Valdes, 2000; Avissar and Werth, 2005).
710 We conclude the following two possibilities in addressing the variations in carbon stocks across
711 the Amazon, but disentangling the contribution of each was beyond the scope of this study. The
712 two models used here incorrectly captured the loss in AGB associated with elevated disturbance,

because they attributed the reduced biomass to changes in either basal area or LAI, which is not well supported in the literature. A second possibility is that disturbance is not a strong indicator of regional variation in AGB, but environmental, community composition, and/or stand structure factors are stronger contributors to regional variation in biomass. Our results showed that a simulated Central Amazon forest that mirrored the turnover of the west and south Amazon continued to differ in multiple forest attributes.

Acknowledgements

We would like to thank Edgard Tribuzy for data collection near the ZF2 research station, and support from the Instituto Nacional de Pesquisas da Amazonia, INPA. We would also like to thank the CESM project, sponsored by the National Science Foundation (NSF) and the U.S. Department of Energy (DOE), and the administration team that is maintained at the National Center for Atmospheric Research (NCAR). This research was supported by the Director, Office of Science, Office of Biological and Environmental Research of the U.S. Department of Energy under contract No. DE-AC02-05CH11231 as part of the Terrestrial Ecosystem Science (TES) Program, and as part of the Earth System Modeling Program (KP170302). This research used resources of the National Energy Research Scientific Computing Center, which is supported by the Office of Science of the U.S. Department of Energy under contract DE-AC02-05CH11231.

References

Anderegg, W. R. L., Kane, J. M., Anderegg, L. D. L.: Consequences of widespread tree mortality triggered by drought and temperature stress, Nature Climate Change, 3, 30-36, 2013.

Avissar, R. and Werth, D.: Global hydroclimatological teleconnections resulting from tropical deforestation. J. of Hydrometer, 6, 134-145, 2005.

Baker, T. R., Phillips, O. L., Malhi, Y., Almeida, S., Arroyo, L., Di Fiore, A., Killeen, T. J., Laurance, S. G., Laurance, W. F., Lewis, S. L., Lloyd, J., Monteagudo, A., Neill, D. A., Patino, S., Pitman, N. C. A., Macedo Silva, J. N., Vasquez Martinez, R.: Variation in wood density determines spatial patterns in Amazonian forest biomass. Global Change Biology, 10, 545–562, 2004a.

Baker, T. R., Phillips, O. L., Malhi, Y., Almeida, S., Arroyo, L., Di Fiore, A., Erwin, T., Higuchi, N., Killeen, T. J., Laurance, S. G., Laurance, W. F., Lewis, S. L., Monteagudo, A., Neill, D. A., Nunez Vargas, P., Pitman, N. C. A., Silva, J. N. M., Vasquez Martinez, R.: Increasing biomass in Amazonian forest plots. Philosophical Transactions of the Royal Society of London, B359, 353–365, 2004b.

Baraloto, C., Rabaud, S., Molto, Q., Blanc, L., Fortunel, C., Herault, B., Davila, N., Mesones, I., Rios, M., Valderrama, E. and Fine, P. V. A.: Disentangling stand and environmental correlates of aboveground biomass in Amazonian forests, Global Change Biology, 17, 2677–2688. doi: 10.1111/j.1365-2486.2011.02432., 2011.

Bonan, G. B.: Forests and climate change: forcings, feedbacks, and the climate benefits of forests. Science, 320, 1444-1449, 2008.

Bondeau, A., Smith, P., Zaehle, S., Schaphoff, S., Lucht, W., Cramer, W., Gerten, D., Lotze-Campen, H., Müller, C., Reichstein, M., Smith, B.: Modelling the role of agriculture for the 20th century global terrestrial carbon balance, Global Change Biology, 13, 679–706, 2007.

Botkin, D. B., Janak, J. F., and Wallis, J. R.: Some Ecological Consequences of a Computer Model of Forest Growth, J. of Ecology, 60, 849-872, 1972.

Brokaw, N. V. L.: Gap-Phase Regeneration in a Tropical Forest, Ecology, 66, 682–687, 1985.

Busing, R. T. and Solomon, A. M.: A comparison of forest survey data with forest dynamics simulators FORCLIM and ZELIG along climatic gradients in Pacific Northwest, Scientific Investigation Report 2004-5078, U.S. Geological Survey, Reston Virginia, USA, 2004.

766 Canadell, J. G., Le Quere, C., Raupach, M. R., Field, C. B., Buitenhuis, E. T., Ciais, P., Conway,
767 T. J., Gillett, N. P., Houghton, R. A., and Marland, G.: Contributions to accelerating atmospheric
768 CO_2 growth from economic activity, carbon intensity, and efficiency of natural sinks, Proc Natl
769 Acad Sci USA, 104, 18866–18870, 2007.
770 Canham, C. D. and Marks, P. L.: The response of woody plants to disturbance: patterns of
771 establishment and growth. The Ecology of Natural Disturbances and Patch Dynamics, Academic
772 Press, New York, NY, 1985.
773 Chambers, J. Q., Higuchi, N., and Schimel, J. P.: Ancient trees in Amazonia, Nature, 391, 135–
774 136, 1998.
775 Chambers, J.Q., Schimel, J. P., and Nobre, A. D.: Respiration from coarse wood litter in central
776 Amazon forests, Biogeochem, 52, 115-131, 2001.
777 Chamber, J. Q., and Silver, W. L.: Some aspects of ecophysiological and biogeochemical
778 responses of tropical forests to atmospheric change, Phil. Trans. R. Soc. Lond. B, 359, 463-476,
779 2004.
780 Chambers, J.Q., Higuchi, N., Teixeira, L. M., dos Santos, J., Laurance, S. G., Trumbore, S. E.:
781 Response of tree biomass and wood litter to disturbance in a Central Amazon forest, Oecologia,
782 141, 596-614, 2004.
783 Chambers, J. Q., Robertson, A., Carneiro, V., Lima, A., Smith, M.-L., Plourde, L., and Higuchi,
784 N.: Hyperspectral remote detection of niche partitioning among canopy trees driven by blowdown
785 gap disturbances in the central Amazon, Oecologia, 160, 107–117, 2009.
786 Chambers, J. Q., Negron-Juarez, R. I., Marra, D. M., Di Vittorio, A., Tews, J., Roberts, D.,
787 Ribeiro, G. H. P. M., Trumbore, S. E., and Higuchi, N.: The steady-state mosaic of disturbance
788 and succession across an old-growth Central Amazon forest landscape, PNAS, 110, 3949-3954,
789 2013.
790 Clark, D. A.: Detecting tropical forests' responses to global climatic an atmospheric change:
791 current challenges and a way forward, Biotropica 39, 4–19, 2007.
792 Chave, J., Riera, B., and Dubois, M. A.: Estimation of biomass in a neotropical forest of French
793 Guiana: spatial and temporal variability, J. of Trop. Ecol., 17, 79–96, 2001.
794 Chave, J., Muller-Landau, Baker, T. R., Easdale, T. A., ter Steege, H., and Webb, C. O.: Regional
795 and phylogenetic variation of wood density across 2456 neotropical tree species, Ecol. Appl., 16,
796 2356-2367, 2006.

797 Collins, W. D., Bitz, C. M., Blackmon, M. L., Bonan, G. B., Bretherton, C. S., Carton, J. A.,
798 Chang, P., Doney, S. C., Hack, J. J., Henderson, T. B., Kiehl, J. T., Large, W. G., McKenna, D.
799 S., Santer, B. D., and Smith, R. D.: The Community Climate System Model version 3 (CCSM3),
800 J. Climate, 19, 2122–2143, 2006.
801 Cox, P. M., Betts, R. A., Jones, C. D., Spall, S.A., Totterdell, I. J.: Acceleration of global
802 warming due to carbon-cycle feedbacks in a coupled climate model, Nature, 408, 184-187, 2000.
803 Cox, P. M., Betts, R. A., Collins, M., Harris, P. P., Huntingford, C., and Jones, C. D.: Amazonian
804 forest dieback under climate-carbon cycle projections for the 21st century, Theoretical and
805 Applied Climatology, 78, 137–156, 2004.
806 Cox, P. M., Pearson, D., Booth, B. B., Friedlingstein, P., Huntingford, C., Jones, C. D., and Luke,
807 C. M.: Sensitivity of tropical carbon to climate change constrained by carbon dioxide variability,
808 Nature, 494, 341-344, 2013.
809 Cramer, W., Bondeau, A., Woodward, F. I., Prentice, I. C., Betts, R. A., Brovkin, V., Cox, P. M.,
810 Fisher, V., Foley, J. A., Friend, A. D., Kucharik, C., Lomas, M. R., Ramankutty, N., Sitch, S.,
811 Smith, B., White, A., and Young-Molling, C.: Global response of terrestrial ecosystem structure
812 and function to CO_2 and cli- mate change: results from six dynamic global vegetation models,
813 Global Change Biol., 7, 357–373, 2001.
814 Cumming, S. G. and Burton, P. J.: A Programmable Shell and Graphics System for Forest Stand
815 Simulation, Environ. Software, 8, 219-230, 1993.
816 Dale, V.H., Joyce, L. A., McNulty, S., Neilson, R. P., Ayers, M. P., Flannigan, M. D., Hanson, P.
817 J., Irland, L. C., Lugo, A. E., Peterson, C. J., Simberloff, D., Swanson, F. J., Stocks, B. J., and
818 Wotton, B. M.: Climate change and forest disturbances, Bioscience, 51, 723-734, 2001.
819 DeFries, R. S., Houghton, R. A., Hansen, M. C., Field, C. B., Skole, D., and Townshend, J.:
820 Carbon emissions from tropical deforestation and regrowth based on satellite observations for the
821 1980s and 1990s, PNAS, 99, 14256-14261, 2002.
822 Denslow J. S.: Tropical rainforest gaps and tree species diversity, Annu. Rev. Ecol. Syst, 18, 431-
823 451, 1987.
824 Fan, S., Gloor, M., Mahlman, J., Pacala, S., Sarmiento, J., Takahashi, T., Tans, P.: A Large
825 Terrestrial Carbon Sink in North America Implied by Atmospheric and Oceanic Carbon Dioxide
826 Data and Models, Science, 282, 442 446, 1998.

827 Fearnside, P. M.: Deforestation in Brazilian Amazonia: History, rates, and consequences, Con-
828 serv. Biol., 19, 680–688, 2005.
829 Franklin, J.F., Shugart, H. H., and Harmon, M. E.: Tree Death as an Ecological Process,
830 BioScience, Vol. 37, No. 8, Tree Death: Cause and Consequence (Sep., 1987), pp. 550-556, 1987.
831 Gedney, N. and Valdes, P. J.: The effect of Amazonian deforestation on the northern hemisphere
832 circulation and climate, Geo. Resear. Lett, 27, 3053-3056, 2000.
833 Gent, P. R., Danabasoglu, G., Donner, L. J., Holland, M. M., hunke, E. C., Jayne, S. R.,
834 Lawrence, D. M., Neale, R. B., Rasch, P. J., Vertenstein, M., Worley, P. H., Yang, Z.-L., and
835 Zhang, M.: The Community Climate System Model version 4, J. Climate, 24, 4973–4991, 2011.
836 Hahmann, A. N., and Dickinson, R. E.: RCCM2-BATS model over tropical South America:
837 Applications to tropical deforestation, J. Climate, 10, 1944–1963, 1997.
838 Henderson-Sellers, A., Dickinson, R.E., Durbidge, T.B., Kennedy, P.J., McGuffie, K., Pitman,
839 A.J.: Tropical deforestation: modelling local to regional-scale climatic change, J. Geophys. Res.
840 98, 7289–7315, 1993.
841 Hirsch, A. I., Little, W. S., Houghton, R. A., Scott, N. A., and White, J. D.: The net carbon flux
842 due to deforestation and forest re-growth in the Brazilian Amazon: analysis using a process-based
843 model, Glob. Change Biol., 10, 908-24, 2004.
844 Holm, J. A., Shugart, H. H., Van Bloem, S.J., and Larocque, G. R.: Gap model development,
845 validation, and application to succession of secondary subtropical dry forests of Puerto Rico,
846 Ecol. Model., 233, 70-82, 2012.
847 Huntingford, C., Zelazowski, P., Galbraith, D., Mercado L. M., Sitch, S., Fisher, R., Lomas, M.,
848 Walker, A. P., Jones, C. D., Booth, B. B. B., Malhi, Y., Hemming, D., Kay, G., Good, P., Lewis,
849 S. L., Phillips, O. L., Atkin, O. K., Lloyd, J., Gloor, E., Zaragoza-Castells, J., Meir, P., Betts, R.,
850 Harris, P. P., Nobre, C., Marango, J., and Cox. P. M.: Simulated resilience of tropical rainforests
851 to CO_2-induced climate change, Nature Geosci, 6, 268-273, 2013.
852 IPCC, Intergovernmental Panel on Climate Change, Climate change 2014: Mitigation of Climate
853 Change. Contribution of working group III to the fifth assessment report of the IPCC, 2014.
854 Jones, A. D., Collins, W. D., Edmonds, J., Torn, M. S., Janetos, A., Calvin, K. V., Thomson, A.,
855 Chini, L. P., Mao, J., Shi, X., Thornton, P., Hurtt, G. C., and Wise, M.: Greenhouse gas policies
856 influence climate via direct effects of land use change, J. Clim., 26, 3657–3670, 2013.

857 Keane, R. E., Austin, M., Field, C., Huth, A., Lexer, M. J., Peters, D., Solomon, A., and Wyckoff,
858 P.: Tree Mortality in Gap Models: Application to Climate Change, Clim. Change 51, 509–540,
859 2001.
860 Keller, M., Palace, M., and Hurtt. G.: Biomass estimation in the Tapajos National Forest, Brazil.
861 Examination of sampling and allometric uncertainties, For. Ecol. and Manage., 154, 371–382,
862 2001.
863 Larocque, G. R., Archambault, L., and Delisle, C.: Modelling forest succession in two
864 southeastern Canadian mixedwood ecosystem types using the ZELIG model, Ecol. Model., 199,
865 350-362, 2006.
866 Larocque, G. R., Archambault, L., and Delisle, C.: Development of the gap model ZELIG-CFS to
867 predict the dynamics of North American mixed forest types with complex structures, Ecol.
868 Model, 222, 2570-2583, 2011.
869 Laurance, W. F. and Williamson, G. B.: Positive feedbacks among forest fragmentation, drought,
870 and climate change in the Amazon, Conser. Bio., 15, 1529-1535, 2001.
871 Laurance, W. F., Fearnside, P. M., Laurance, S. G., Delamonica, P., Lovejoy, T. E., Rankin-de
872 Merona, J. M., Chambers, J. Q., and Gascon, C.: Relationship between soils and Amazon forest
873 biomass: a landscape-scale study, For. Ecol. and Manage., 118, 127-138, 1999.
874 Laurance, W.F., Nascimento, H. E. M., Laurance, S. G., Condit, R., D'Angelo, S., Andrade, A.:
875 Inferred longevity of Amazonian rainforest trees based on a long-term demographic study, For.
876 Ecol. and Manage., 190, 131-143, 2004.
877 Lawrence, D. M., Oleson, K. W., Flanner, M. G., Thornton, P. E., Swenson, S. C., Lawrence, P.
878 J., Zeng, X., Yang, Z.-L., Levis, S., Sakaguchi, K., Bonan, G. B., and Slater, A. G.:
879 Parameterization improvements and functional and structural advances in version 4 of the
880 Community Land Model, J. Adv. Model. Earth Syst., 3, M03001, 2011.
881 Le Page, Y., Hurtt G., Thomson A.M., Bond-Lamberty B., Patel P., Wise M., Calvin K., Kyle P.,
882 Clarke L., Edmonds J., Janetos A.: Sensitivity of climate mitigation strategies to natural
883 disturbances, Environ. Res. Lett., 8, 015018, 2013.
884 Lewis, S. L. Phillips, O. L., Baker, T. R., Lloyd, J., Malhi, Y., Almeida, S., Higuchi, N.,
885 Laurance, W. F., Neill, D. A., Silva, J. N. M., Terborgh, J., Torres Lezama, A., Vasquez
886 Martinez, R., Brown, S., Chave, J., Kuebler, C., Nunez Vargas P., and Vinceti, B.: Concerted

887 changes in tropical forest structure and dynamics: evidence from 50 South American long-term
888 plots, Phil. Trans. R. Soc. Lond. B., 359, 421–436, 2004.
889 Lewis, S. L., Brando, P. M., Phillips, O. L., van der Heijden, G. M. F., and Nepstad, D.: The 2010
890 Amazon drought, Science, 331, 554, 2011.
891 Lieberman, D., Lieberman, M., Peralta, R., and Hartshorn, G. S.: Mortality Patterns and Stand
892 Turnover Rates in a Wet Tropical Forest in Costa Rica, J. of Ecology, 73, 915-924, 1985.
893 Lutz, D. A., Shugart, H. H., White, M. A.: Sensitivity of Russian forest timber harvest and carbon
894 storage to temperature increase, Forestry, 86, 283-293, 2013.
895 Mailly, D., Kimmins, J. P., Busing, R. T.: Disturbance and succession in a coniferous forest of
896 northwestern North America: simulation with DRYADES, a spatial gap model, Ecol. Model, 127,
897 183–205, 2000.
898 Malhi, Y., and Phillips, O. L.: Tropical forests and global atmospheric change: a synthesis, Philos.
899 Trans. R. Soc. Lond. B. Biol. Sci., 359, 549–555, 2004.
900 Malhi, Y., Phillips, O. L., Lloyd, J., Baker, T., Wright, J., Almeida, S., Arroyo, L., Frederiksen,
901 T., Grace, J., Higuchi, N., Killeen, T., Laurance, W. F., Leaño, C., Lewis, S., Meir,
902 P., Monteagudo, A., Neill, D., Núñez Vargas, P., Panfil, S. N., Patiño, S., Pitman, N.,Quesada, C.
903 A., Rudas-Ll, A., Salomão, R., Saleska, S., Silva, N., Silveira, M., Sombroek, W. G., Valencia,
904 R., Vásquez Martínez, R., Vieira, I. C. G. and Vinceti, B.: An international network to monitor
905 the structure, composition and dynamics of Amazonian forests (RAINFOR). J. of Veg.
906 Sci. 13, 439–450, 2002.
907 Malhi, Y., Wood, D., Baker, T. R., Wright, J., Phippips, O. L., Cochrane, T., Meir, P., Chave J.,
908 Almeida, S., Arroyo, L., Higuchi, N., Killeen, T. J., Laurance, S. G., Laurance, W. F., Lewis, S.
909 L., Monteagudo, A., Neill, D. A., Vargas, P. N., Pitman, N. C. A., Quesada, C. A., Salomao, R.,
910 Silva, J. N. M., Lezama, A. T., Terborgh, J., Martinez, R. V. and Vinceti, B.: The regional
911 variation of aboveground live biomass in old-growth Amazonian forests, Global Change Biology,
912 12, 1107–1138. doi: 10.1111/j.1365-2486.2006.01120.x, 2006.
913 Malhi, Y., Timmons Roberts, J., Betts, R. A., Killeen, T. J., Li, W., Nobre, C. A.: Climate change,
914 deforestation, and the fate of the Amazon, Science, 319, 169-172, 2008.
915 Malhi, Y., Aragão, L. E. O. C., Galbraith, D., Huntingford, C., Fisher, R., Zelazowski, P., Sitch,
916 S., McSweeney, C., and Meir, P.: Exploring the likelihood and mechanism of a climate-change-
917 induced dieback of the Amazon rainforest, Proc. Nat. Acad. Sci. USA, 106, 20610–20615, 2009.

McDowell, N. G.: Mechanisms linking drought, hydraulics, metabolism, and vegetation mortality, Plant Phys., 155, 1051-1059, 2011.

McDowell, N., Pockman, W. T., Allen, C. D., Breshears, D. D., Cobb, N., Kolb, T., Plaut, J., Sperry, J., West, A., Williams, D. G., and Yepez, E. A.: Mechanisms of plant survival and mortality during drought: Why do some plants survive while others succumb to drought?, New Phytol.. 178, 719–739, 2008.

Miller, S. D., Goulden, M. L., Menton, M. C., Da Rocha, H. R., De Freitas, H. C., Silva Figueira, A. M. E., and Dias de Sousa, C. A.: Biometric and micrometeorological measurements of tropical forest carbon balance, Ecol. App., 14, S114-S126, 2003.

Morton, D. C., DeFries, R. S., Shimabukuro, Y. E., Anderson, L. O., Arai, E., del Bon Espirito-Santo, F., Freitas, R., and Morisette, J.: Cropland expansion changes deforestation dynamics in the southern Brazilian Amazon, Proc. Nat. Acad. Sci. USA, 103, 14637-14641, 2006.

Muller-Landau, H. C.; Interspecific and intersite variation in wood specific gravity of tropical trees, Biotropica, 36, 20-32, 2004.

Nakayama, T.: Shrinkage of shrub forest and recovery of mire ecosystem by river restoration in northern Japan, For. Ecol. and Manage., 256, 1927-1938, 2008.

Negrón-Juárez, R. I., Chambers, J. Q., Guimaraes, G., Zeng, H., Raupp, C. F. M., Marra, D. M., Ribeiro, G. H. P. M., Saatchi, S. S., Nelson, B. W., and Higuchi, N.: Widespread Amazon forest tree mortality from a single cross-basin squall line event, Geo. Res. Letters 37, L16701, 2010.

Nepstad, D. C., Tohver, I. M., Ray, D., Moutinho, P., and Cardinot, G.: Mortality of large trees and lianas following experimental drought in an Amazon forest, Ecology, 88, 2259–2269, 2007.

Nogueira, E. M., Nelson, B. W., Fearnside, P. M.: Wood density in dense forest in central Amazonia, Brazil, For. Ecol. Manage., 208, 261-286, 2005.

Norby, R. J., DeLucia, E. H., Gielen, B., Calfapietra, C., Giardina, C. P., King, J. S., Ledford, J., McCarthy, H. R., Moore, D. J. P., Ceulemans, R., De Angelis, P., Finzi, A. C., Karnosky, D. F., Kubiske, M. E., Lukac, M., Pregitzer, K. S., Scarascia-Mugnozza, G. E., Schlesinger, W. H., and Oren, R.: Forest response to elevated CO_2 is conserved across a broad range of productivity, Proc. Natl. Acad. Sci., 102, 18052–18056, 2005.

Norby. R. J., Warren, J. M., Iverson, C. M., Medlyn, B. E., and McMurtrie, R. E.: CO_2 enhancement of forest productivity constrained by limited nitrogen availability, Proc. Natl. Acad. Sci., 107, 19368-19373, 2010.

O'Brien, S. T., Hayden, B. P., and Shugart, H. H.: Global change, hurricanes and a tropical Forest, Climatic Change, 22, 175-190, 1992.

Oleson, K. W., Lawrence, D. M., Bonan, G. B., Flanner, M. G., Kluzek, E., Lawrence, P. J., Levis, S., Swenson, S. C., and Thornton, P. E.: Technical description of version 4.0 of the Community Land Model (CLM), NCAR Tech. Note NCAR/TN-478+STR, 257 pp., 2010.

Overpeck, J. T., Rind, D., and Goldberg, R.: Climate-induced changes in forest disturbance and vegetation, Nature, 343, 51-53, 1990.

Pan, Y., Birdsey, R. A., Fang, J., Houghton, R., Kauppi, P. E., Kurz, W.A., Phillips, O. L., Shvidenko, A., Lewis, S. L., Canadell, J. G., Ciais, P., Jackson, R. B., Pacala, S. W., McGuire, A. D., Piao, S., Rautiainen, A., Sitch, S., and Hayes, D.: A large and persistent carbon sink in the world's forests, Science 333, 988–993, 2011.

Patiño, S., Lloyd, J., Paiva, R., Baker, T. R., Quesada, C. A., Mercado, L. M., Schmerler, J., Schwarz, M., Santos, A. J. B., Aguilar, A., Czimczik, C. I., Gallo, J., Horna, V., Hoyos, E. J., Jimenez, E. M., Palomino, W., Peacock, J., Peña-Cruz, A., Sarmiento, C., Sota, A., Turriago, J. D., Villanueva, B., Vitzthum, P., Alvarez, E., Arroyo, L., Baraloto, C., Bonal, D., Chave, J., Costa, A. C. L., Herrera, R., Higuchi, N., Killeen, T., Leal, E., Luizão, F., Meir, P., Monteagudo, A., Neil, D., Núñez-Vargas, P., Peñuela, M. C., Pitman, N., Priante Filho, N., Prieto, A., Panfil, S. N., Rudas, A., Salomão, R., Silva, N., Silveira, M., Soares deAlmeida, S., Torres-Lezama, A., Vásquez-Martínez, R., Vieira, I., Malhi, Y., and Phillips, O. L.: Branch xylem density variations across the Amazon Basin, Biogeosciences, 6, 545-568, doi:10.5194/bg-6-545-2009, 2009.

Phillips, O. L., Malhi, Y., Higuchi, N., Laurance, W. F., Nuñez, P. V., Vásquez, R. M., Laurance, S. G., Ferreira, L. V., Stern, M., Brown, S., and Grace, J.: Changes in the carbon balance of tropical forests: evidence from long-term plots, Science, 282, 439–442, 1998.

Phillips, O. L., Baker, T. R., Arroyo, L., Higuchi, N., Killeen, T. J., Laurance, W. F., Lewis, S. L., Lloyd, J., Malhi, Y., Monteagudo, A., Neill, D. A., Vargas, P. N., Silva, J. N., Terborgh, J., Martínez, R. V., Alexiades, M., Almeida, S., Brown, S., Chave, J., Comiskey, J. A., Czimczik, C. I., Di Fiore, A., Erwin, T., Kuebler, C., Laurance, S. G., Nascimento, H. E., Olivier, J., Palacios, W., Patiño, S., Pitman, N. C., Quesada, C. A., Saldias, M., Lezama, A. T., and Vinceti, B.: Pattern and process in Amazon tree turnover, 1976–2001, Philos. Trans. R. Soc. Lond. B. Biol. Sci., 359, 381–407, 2004.

Phillips, O. L., Lewis, S. L., Baker, T. R., Chao, K.-J., and Higuchi, N.: The changing Amazon forest, Phil. Trans. R. Soc. B., 363,1819-1827, 2008.

Phillips, O. L., Aragão, L. E. O. C., Lewis, S. L., Fisher, J. B., Lloyd, J., López-González, G., Malhi, Y., Monteagudo, A., Peacock, J., Quesada, C. A., van der Heijden, G., Almeida, S., Amaral, I., Arroyo, L., Aymard, G., Baker, T. R., Ba´nki, O., Blanc, L., Bonal, D., Brando, P., Chave, J., Alves de Oliveira, A´. C., Dávila Cardozo, N., Czimczik, C. I., Feldpausch, T. R., Freitas, M. A., Gloor, E., Higuchi, N., Jiménez, E., Lloyd, G., Meir, P., Mendoza, C., Morel, A., Neill, D. A., Nepstad, D., Patiño, S., Peñuela, M. C., Prieto, A., Ramírez, F., Schwarz, M., Silva, J., Silveira, M., Sota Thomas, A., ter Steege, H., Stropp, J., Vásquez, R., Zelazowski, P., Alvarez Dávila, E., Andelman, S., Andrade, A., Chao, K., Erwin, T., Di Fiore, A., Honorio, C., Keeling, E., Killeen, H., Laurance, T. J., Peña Cruz, W. F., Pitman, A., Núñez Vargas, N. C. A., Ramírez-Angulo, P., Rudas, H., Salamão, A., Silva, R., Terborgh, N., Torres- Lezama, J. A.: Drought sensitivity of the Amazon rainforest, Science, 323, 1344–1347, 2009.

Quesada, C. A., Lloyd, J., Schwarz, M., Patiño, S., Baker, T. R., Czimczik, C., Fyllas, N. M., Martinelli, L., Nardoto, G. B., Schmerler, J., Santos, A. J. B., Hodnett, M. G., Herrera, R., Luizão, F. J., Arneth, A., Lloyd, G., Dezzeo, N., Hilke, I., Kuhlmann, I., Raessler, M., Brand, W. A., Geilmann, H., Moraes Filho, J. O., Carvalho, F. P., Araujo Filho, R. N., Chaves, J. E., Cruz Junior, O. F., Pimentel, T. P., and Paiva, R.: Variations in chemical and physical properties of Amazon forest soils in relation to their genesis, Biogeosciences, 7, 1515-1541, 2010.

Rammig, A., Jupp, T., Thonicke, K., Tietjen, B., Heinke, J., Ostberg, S., Lucht, W., Cramer, W., and Cox, P.: Estimating the risk of Amazonian forest dieback, New Phytologist, 187, 694-706, 2010.

Rice, A. H., Pyle, E. H., Saleska, S. R., Hutyra, L. R., Palace, M., Keller, M., De Camargo, P. B., Portilho, K., Marques, D. F., and Wofsy, S. C.: Carbon balance and vegetation dynamics in an old-growth Amazonian forest, Ecol. Appl., 14, S55–S71, 2004.

Saatchi, S., Malhi, Y., Zutta, B., Buermann, W., Anderson, L. O., Araujo, A. M., Phillips, O. L., Peacock, J., ter Steege, H., Lopez Gonzalez, G., Baker, T., Arroyo, L., Almeida, S., Higuchi, N., Killeen, T., Monteagudo, A., Neill, D., Pitman, N., Prieto, A., Salomão, R., Silva, N., Vásquez Martínez, R., Laurance, W., and Ramírez, H. A.: Mapping landscape scale variations of

1010 forest structure, biomass, and productivity in Amazonia, Biogeosciences Discuss., 6, 5461-5505,
1011 doi:10.5194/bgd-6-5461-2009, 2009.
1012 Sanford, R. L. Jr.: Fine root biomass under light gap openings in an amazon rain forest,
1013 Oecologia, 83, 541-545, 1990.
1014 Seagle, S. W., and Liang, S.: Application of a forest gap model for prediction of browsing effects
1015 on riparian forest succession, Ecol. Model., 144, 213-229, 2001.
1016 Sitch, S., Smith, B., Prentice, I. C., Arneth, A., Bondeau, A., Cramer, W., Kaplan, J. O., Levis, S.,
1017 Lucht, W., Sykes, M. T., Thonicke, K., and Venevsky, S.: Evaluation of ecosystem dy- namics,
1018 plant geography and terrestrial carbon cycling in the LPJ Dynamic Global Vegetation Model,
1019 Global Change Biol., 9, 161–185, 2003.
1020 Shugart, H. H.: A theory of forest dynamics, Springer-Verlag, New York, USA, 1984.
1021 Shugart, H. H.: Forest Gap Models. Vol. 2, The Earth system: biological and ecological
1022 dimensions of global environmental change, Eds. H. A. Mooney and J. C. Canadell in
1023 Encyclopedia of Global Environmental Change, John Wiley & Sons, pp. 316- 323, 2002.
1024 Shugart, H. H. and West, D. C.: Development of an Appalachian Deciduous Forest Succession
1025 Model and its Application to Assessment of the Impact of the Chestnut Blight, J. of Environ.
1026 Manage., 5, 161-179, 1977.
1027 Shugart, H. H., Smith, T. M. and Post, W. M.: The potential for application of individual-based
1028 simulation models for assessing the effects of global change, Ann. Rev. of Eco. and Systematics,
1029 23, 15-38, 1992.
1030 Shukla, J., Nobre, C., and Sellers, P.: Amazon deforestation and climate change, Science, 247,
1031 1322-1325, 1990.
1032 Shuman, J. K., Shugart, H. H., and O'Halloran, T. L.: Sensitivity of Siberian larch forests to
1033 climate change, Glob. Change Biol., 17, 2370–84, 2011.
1034 Smith, J. B., and Tirpak, D. A.: Eds. The potential effects of global climate change on the U.S.:
1035 Appendix D – Forest. Off. Policy, Planning Eval. Washington, DC: US Environ. Protection
1036 Agency, 1989.
1037 Smith, B., Prentice, C. I., and Sykes, M. T.: Representation of vegetation dynamics in the
1038 modelling of terrestrial ecosystems: comparing two contrasting approaches within European
1039 climate space, Global Ecol. and Biogeo., 10, 621-637, 2001.

1040 Smith, T. M. and Urban, D. L.: Scale and the resolution of forest structural pattern, Vegetatio, 74,
1041 143-150, 1988.
1042 Solomon, A. M.: Transient response of forests to CO2-induced climate change: Simulations
1043 experiments in eastern North America, Oecologia, 68, 567-579, 1986.
1044 Suzuki, E.: Diversity in specific gravity and water content of wood among Bornean tropical
1045 rainforest trees, Ecol. Res., 14, 211–224, 1999.
1046 ter Steege, H., Pitman, N. C. A., Phillips, O. L., Chave, J., Sabatier, D., Duque, A., Molion, J.-F.,
1047 Prevost, M.-F., Spichiger, R., Castellanos, H., von Hildebrand, P., and Vasquez, R.: Continental-
1048 scale patterns of canopy tree composition and function across Amazonia, Nature, 443, 444-447,
1049 2006.
1050 Tribuzy, E. S.: Variacoes da temperature foliar do dossel e o seu efeito na taxa assimilatoria de
1051 CO_2 na Amazonia Central, Master's Thesis, Escola Superior de Agricultura "Luiz de Queiroz",
1052 Universidade de Sao Paulo, 2005.
1053 Thonicke, K., Spessa, A., Prentice, I. C., Harrison, S. P., Dong, L., and Carmona-Moreno, C.: The
1054 influence of vegetation, fire spread and fire behaviour on biomass burning and trace gas
1055 emissions: results from a process-based model, Biogeosci., 7, 1991-2011, 2010.
1056 Thornton, P. E., Law, B. E., Gholz, H. L., Clark, K. L., Falge, E., Ellsworth, D. S., Goldstein, A.
1057 H., Monson, R. K., Hollinger, D., Falk, M., Chen, J., and Sparks, J. P.: Modeling and measuring
1058 the effects of disturbance history and climate on carbon and water budgets in evergreen needleleaf
1059 forests, Agric. For. Meteor., 113, 185-222, 2002.
1060 Thornton, P. E., Lamarque, J.-F., Rosenbloom, N. A., and Mahowald, N. M.: Influence of carbon-
1061 nitrogen cycle coupling on land model response to CO2 fertilization and climate variability, Glob.
1062 Biogeochem. Cyc., 21, GB4018, 2007.
1063 Uhl C.: Tree dynamics in a species rich forest tierra firme forest in Amazonia, Venezuela, Acta
1064 Cientifica Venezolana, 33, 72-77, 1982.
1065 Urban, D. L.: A Versatile Model to Simulate Forest Pattern: A User's Guide to ZELIG Version 1.
1066 0, University of Virginia, Charlottesville, Virginia, 1990.
1067 Urban, D. L.: Using model analysis to design monitoring programs for landscape management
1068 and impact assessment, Ecol. Appl., 10, 1820−1832, 2000.
1069 Urban, D. L., Bonan, G. B., Smith, T. M., Shugart, H. H.: Spatial applications of gap models, For.
1070 Ecol. Manage., 42, 95–110, 1991.

1071 Urban, D. L., Harmon, M. R., and Halpern, C. B.: Potential Response of Pacific Northwestern
1072 Forests to Climatic Change, Effects of Stand Age and Initial Composition, Clim. Change, 23,
1073 247-266, 1993.
1074 U.S. DOE: Research Priorities for Tropical Ecosystems Under Climate Change Workshop Report,
1075 DOE/SC-0153, U.S. Department of Energy Office of Science. science.energy.gov/ber/news-and-
1076 resources/, 2012.
1077 Van Daalen, J. C., and Shugart, H. H.: OUTENIQUA – A computer model to simulate succession
1078 in the mixed evergreen forests of southern Cape, South Africa, Landscape Ecology, 2, 255-267,
1079 1989.
1080 Whitmore, T. C.: An introduction to tropical rain forests, Oxford University Press, NewYork,
1081 1989.
1082 Wirth, R., Weber, B., and Ryel, R. J.: Spatial and temporal variability of canopy structure in a
1083 tropical moist forest, Acta Oecologia, 22, 235-244, 2001.
1084 Yang, X., Thornton, P. E., Ricciuto, D. M., and Post, W. M.: The role of phosphorus dynamics in
1085 tropical forests – a modeling study using CLM-CNP, Biogeoscience Discuss., 10, 14439-14473,
1086 2013.
1087 Zhou, X., Fu, Y., Zhou, L., and Luo, Y.: An imperative need for global change research in
1088 tropical forests, Tree Physiol., 33, 903-912, 2013.

Table 1. Species-specific allometric and ecological parameters for the 90 tree species used in ZELIG-TROP, representing species found in central Amazonian (Laurance et al. 2004). All species were assigned a probability factor of stress mortality of 0.369, probability factor of natural mortality of 2.813, zone of seed influence of 200, relative seedling establishment rate (RSER) of 0.9, a crown shape value of 4.0, tolerance to drought a ranking of 3, tolerance to low soil nutrients a ranking of 2, minimum growing degree-day of 5000, and a maximum growing degree-day of 12,229.50.

Species	Growth Form	AGE-MAX (yr)	DBH max (cm)	HT max (cm)	G.	L.	Stock (%)	Wood Density (g cm^{-3})
Anacardium spruceanum	Canopy	175	69.1	3620.4	75.2	2	0.8	0.46
Aniba canelilla	Canopy	226	37.8	2032.8	38.7	2	0.5	0.94
Aspidosperma marcgravianum	Emergent	544	90.0	4680.4	30.8	4	0.5	0.72
Aspidosperma oblongum	Emergent	331	80.0	4173.2	59.5	4	0.5	0.87
Astronium le-cointei	Canopy	335	50.0	2651.6	34.7	2	0.5	0.77
Bocageopsis multiflora	Canopy	152	33.1	1794.5	51.3	2	0.5	0.65
Brosimum acutifolium	Canopy	264	58.3	3072.6	36.2	2	0.5	0.62
Brosimum guianense	Canopy	477	60.0	3158.8	22.3	2	0.5	0.89
Brosimum parinarioides	Canopy	483	60.0	3158.8	24.9	2	0.5	0.62
Brosimum rubescens	Canopy	450	60.0	3158.8	27.1	2	0.5	0.84
Cariniana micrantha	Emergent	223	80.0	4173.2	76.5	4	0.5	0.60
Caryocar glabrum	Canopy	527	110.0	5694.8	32.1	2	0.5	0.71
Casearia arborea	Canopy	91	20.1	1135.1	39.1	2	0.8	0.57
Casearia sylvestris	Canopy	201	25.5	1409.0	23.7	2	0.5	0.71
Clarisia racemosa	Canopy	323	80.0	4173.2	44.7	2	0.5	0.57
Cordia sagotli	Subcanopy	260	26.3	1449.6	14.6	1	0.8	0.43
Corythophora rimosa	Canopy	235	50.0	2651.6	48.1	2	0.5	0.81
Couepia longipendula	Canopy	260	46.6	2479.2	37.7	2	0.5	0.94
Couma macrocarpa	Canopy	233	51.8	2742.9	56.8	2	0.8	0.50
Couratari stellata	Emergent	592	53.5	2829.1	13.4	4	0.5	0.63
Dipteryx odorata	Emergent	323	78.4	4092.1	47.7	4	0.5	0.92
Drypetes variabilis	Subcanopy	252	30.0	1637.2	23.7	1	0.5	0.73
Duckeodendron cestroides	Emergent	818	140.0	7216.4	18.8	4	0.5	0.63
Ecclinusa guianensis	Canopy	448	69.7	3650.8	28.5	2	0.5	0.63
Endopleura uchi	Canopy	223	57.6	3037.1	52.5	2	0.5	0.79
Eriotheca globosa	Canopy	135	20.1	1135.1	28.3	2	0.8	0.41
Eschweilera amazoniciformis	Emergent	369	56.1	2961.0	30.5	4	0.5	0.82

Eschweilera coriacea	Canopy	767	110.0	5694.8	25.7	2	0.5	0.84
Fusaea longifolia	Subcanopy	413	26.5	1459.7	11.5	1	0.5	0.74
Glycydendron amazonicum	Canopy	386	44.0	2347.3	23.8	2	0.5	0.67
Goupia glabra	Emergent	398	100.0	5187.6	44.7	4	0.5	0.72
Guatteria olivacea	Canopy	54	30.0	1637.2	126.4	2	0.8	0.47
Gustavia elliptica	Subcanopy	301	24.7	1368.4	16.8	1	0.5	0.67
Helicostylis tomentosa	Canopy	311	44.7	2382.8	24.0	2	0.5	0.63
Hevea guianensis	Canopy	288	45.7	2433.5	29.3	2	0.5	0.55
Inga capitata	Pioneer	162	26.4	1454.6	27.6	3	0.7	0.60
Inga paraensis	Pioneer	78	40.0	2144.4	95.2	3	0.7	0.82
Inga splendens	Pioneer	52	38.2	2053.1	157.6	3	0.7	0.58
Iryanthera juruensis	Subcanopy	569	26.9	1480.0	8.8	1	0.5	0.66
Iryanthera laevis	Subcanopy	331	27.2	1495.2	15.4	1	0.5	0.63
Jacaranda copaia	Pioneer	225	30.0	1637.2	21.0	3	0.8	0.35
Lecythis barnebyi	Subcanopy	336	28.7	1571.3	19.9	1	0.5	0.82
Lecythis poiteaui	Canopy	747	34.4	1860.4	7.7	2	0.5	0.80
Lecythis zabucajo	Emergent	628	130.0	6709.2	27.0	4	0.5	0.86
Licania apetala	Canopy	199	38.4	2063.3	37.8	2	0.5	0.76
Licania oblongifolia	Canopy	196	54.2	2864.6	65.7	2	0.5	0.88
Licania octandra	Subcanopy	339	35.0	1890.8	21.7	1	0.5	0.81
Licania cannella	Canopy	359	56.5	2981.3	29.0	2	0.5	0.79
Macrolobium angustifolium	Canopy	335	40.0	2144.4	27.7	2	0.5	0.68
Manilkara bidentata	Emergent	773	90.0	4680.4	20.6	4	0.5	0.87
Manilkara huberi	Emergent	349	100.0	5187.6	55.9	4	0.5	0.93
Maquira sclerophylla	Emergent	420	60.0	3158.8	24.0	4	0.5	0.53
Mezilaurus itauba	Canopy	684	44.0	2347.3	12.9	2	0.5	0.74
Micropholis guyanensis	Canopy	248	55.5	2930.6	45.9	2	0.5	0.66
Micropholis venulosa	Canopy	491	60.0	3158.8	22.9	2	0.5	0.67
Minquartia guianensis	Emergent	490	70.0	3666.0	30.4	4	0.5	0.77
Myrciaria floribunda	Subcanopy	490	29.1	1591.6	11.7	1	0.5	0.77
Onychopetalum amazonicum	Canopy	195	29.9	1632.1	33.0	2	0.5	0.61
Parkia multijuga	Emergent	206	119.0	6151.3	101.7	4	0.8	0.39
Peltogyne paniculata	Canopy	251	40.0	2144.4	28.0	2	0.5	0.80
Pourouma bicolor	Pioneer	48	29.8	1627.1	124.6	3	0.8	0.38
Pourouma guianensis	Pioneer	58	31.3	1703.2	112.8	3	0.8	0.38
Pouteria ambelaniifolia	Canopy	296	38.0	2043.0	21.0	2	0.5	0.70
Pouteria anomala	Emergent	452	70.0	3666.0	31.6	4	0.5	0.78
Pouteria caimito	Canopy	240	43.2	2306.7	36.4	2	0.5	0.82
Pouteria eugeniifolia	Canopy	329	44.1	2352.4	25.8	2	0.5	1.10
Pouteria guianensis	Canopy	720	80.0	4173.2	17.5	2	0.5	0.94
Pouteria macrophylla	Canopy	387	29.6	1616.9	13.2	2	0.5	0.86
Pouteria manaosensis	Canopy	981	50.0	2651.6	8.4	2	0.5	0.64
Pouteria multiflora	Canopy	547	35.5	1916.2	9.5	2	0.5	0.75

Pouteria oppositifolia	Canopy	277	35.8	1931.4	21.7	2	0.5	0.65
Pouteria venosa	Canopy	702	45.8	2438.6	10.0	2	0.5	0.92
Protium altsonii	Emergent	238	70.0	3666.0	56.4	4	0.5	0.68
Protium decandrum	Canopy	158	32.8	1779.2	40.3	2	0.5	0.52
Protium heptaphyllum	Canopy	96	26.2	1444.5	60.0	2	0.8	0.62
Protium tenuifolium	Canopy	170	38.2	2053.1	49.1	2	0.5	0.57
Qualea paraensis	Emergent	379	70.0	3666.0	31.9	4	0.5	0.67
Scleronema micranthum	Emergent	353	90.0	4680.4	50.3	4	0.5	0.60
Sloanea guianensis	Subcanopy	179	28.5	1561.1	26.8	1	0.5	0.82
Swartzia corrugata	Subcanopy	407	21.1	1185.8	7.7	1	0.5	1.06
Swartzia recurva	Canopy	177	38.4	2063.3	45.5	2	0.5	0.97
Swartzia ulei	Canopy	293	50.0	2651.6	39.1	2	0.5	1.00
Tachigali paniculata	Canopy	91	27.7	1520.6	60.1	2	0.8	0.56
Tapirira guianensis	Canopy	54	41.6	2225.6	188.0	2	0.8	0.45
Tetragastris panamensis	Canopy	320	38.4	2063.3	25.1	2	0.5	0.72
Vantanea parviflora	Canopy	205	69.6	3645.7	65.1	2	0.5	0.84
Virola calophylla	Subcanopy	293	30.8	1677.8	18.6	3	0.8	0.51
Virola multinervia	Canopy	373	32.0	1738.7	14.0	2	0.8	0.45
Virola sebifera	Canopy	161	30.2	1647.4	44.4	2	0.8	0.46
Vochysia obidensis	Canopy	92	47.4	2519.7	109.1	2	0.8	0.50

Key: AGEMAX, maximum age for the species (yr); DBHmax, maximum diameter at breast height (cm); HTmax, maximum height (cm); G, growth rate scaling coefficient (unitless); Light (L): light/shade tolerance class (ranking 1-5); Stock, regeneration stocking (%), wood density (g cm^{-3}); (full parameter explanation found in original ZELIG paper: Urban 1990).

1100 **Table 2**. Environmental parameters used in ZELIG-TROP for the central Amazon basin. Values

1101 reported in a range were monthly low and high averages. *Lawrence et al., (1999).

Lat./Long./Alt. (m)	Plot Area (m^2)	Mean monthly temperature (˚C)	Mean monthly precipitation (cm)	Soil field capacity (cm)*	Soil wilting point (cm)*	Relative direct and diffuse solar radiation (%)
-2.3/-60.0/100.0	400.0	25.18 - 27.47	8.01 - 45.16	52.0	32.9	0.6/0.4

1102

Table 3. Averages (and standard deviations) of five forest attributes for the observed values recorded from sites near Manaus, Brazil, averaged over 5 ha, and the modeled ZELIG-TROP results. ZELIG-TROP results are averaged for the final 100 years, after an initial spin up of 400 years. The remaining values correspond to the percent differences between the observed and simulated values, and the minimum and maximum range of a ZELIG-TROP simulation.

	Avg. Basal Area (m^2 ha^{-1})	Avg. Biomass (Mg C ha^{-1})	Avg. Stem Density (ha^{-1})	Avg. LAI	Avg. ANPP (Mg C ha^{-1} yr^{-1})
Empirical Data	30.06 (6.61)	169.84 (27.60)	656 (22)	5.7 (0.50)	6.5
ZELIG-TROP	32.96 (1.22)	178.38 (10.53)	574 (70)	5.8 (0.24)	5.4 (0.22)
Percent Diff. (%)	9.66	5.03	-12.49	1.75	-17.08
ZELIG-TROP min./max.	31.14/35.97	167.97/189.26	472/688	5.26/6.48	5.08/5.92

1109 **Table 4**. Comparison of empirical data and stand model data from Chambers et al. (2004) unless
1110 otherwise noted, ZELIG-TROP pre- and post-disturbance treatments, and CLM pre- and post-
1111 disturbance treatments for the pool of carbon in live trees, and the annual flux of carbon from
1112 stem growth, coarse litter production rates from mortality, ANPP; and recruitment rate of stems,
1113 mean DBH, and average ΔAGB.

Positive = sink	Live Trees (Mg C ha^{-1})	Growth (Mg C ha^{-1} yr^{-1})	Coarse Litter (Mg C ha^{-1} yr^{-1})	ANPP (Mg C ha^{-1} yr^{-1})	Recruitment (% yr^{-1})	Mean DBH (cm)	AGB change (Mg C ha^{-1} yr^{-1})
Empirical[§]	156	1.70	-2.10	6.50*	1.38**	21.1	NA
Stand Model[§]	160	1.60	-1.70	6.60	NA	20.4	NA
ZELIG-TROP[1]	178	3.09	-3.03	5.39	2.33	22.3	0.02
ZELIG-TROP[2]	104	2.89	-2.78	5.35	3.94	18.3	0.01
ZELIG-TROP[3]	138	3.29	-3.49	5.06	3.41	26.9	-0.15
CLM-CN[1]	269	4.88	-4.82	7.81	NA	NA	0.04
CLM-CN[2]	135	4.91	-4.93	7.83	NA	NA	0.00
CLM-CN[3]	230	4.71	-4.95	7.54	NA	NA	-0.46
ZELIG Diff. (1&2)	-74	-0.20	0.25	-0.04	1.61	-4.0	0.01
ZELIG Diff. (1&3)	-40	0.20	-0.46	-0.33	1.08	4.6	-0.17
CLM Diff. (1&2)	-134	0.03	-0.11	0.02	NA	NA	-0.04
CLM Diff. (1&3)	-39	-0.17	-0.15	-0.27	NA	NA	-0.50

1114 1 = No Disturbance, 2 = High Disturbance, 3 = Periodic Disturbance, § Chambers et al. (2004), * Chambers et al. (2001), **
1115 Phillips et al. (2004).

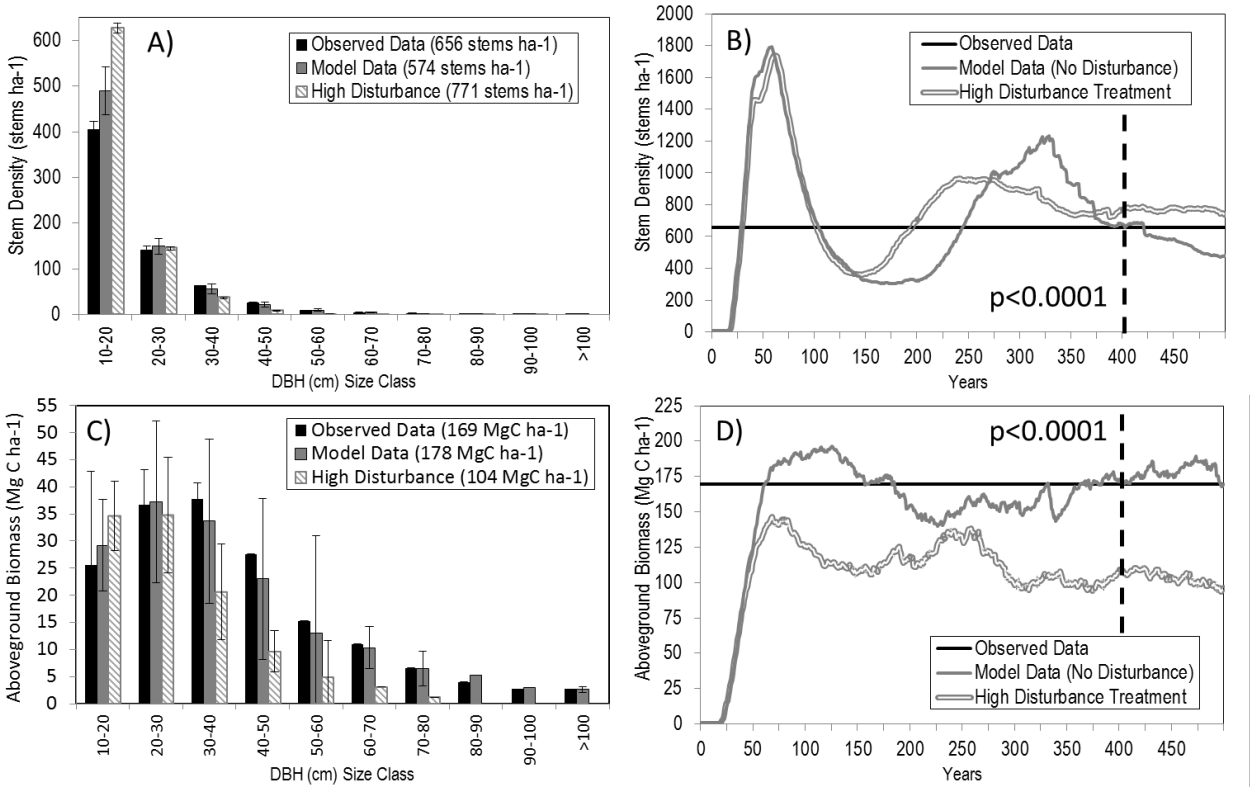

Fig. 1. Comparison between observed field data from "transects" in Central Amazon, ZELIG-TROP model data from no-disturbance scenario, and ZELIG-TROP model data from high-disturbance treatment. **(A)** Average stem density (stems ha^{-1}) and SD by DBH (cm) size class, **(B)** stem density simulated over 500 years, **(C)** average above-ground biomass (Mg ha^{-1}) and SD by DBH (cm) size class, and **(D)** above-ground biomass simulated over 500 years. Average results and t-test between two model results taken once the model reached a steady-state, or the final 100 years of simulation.

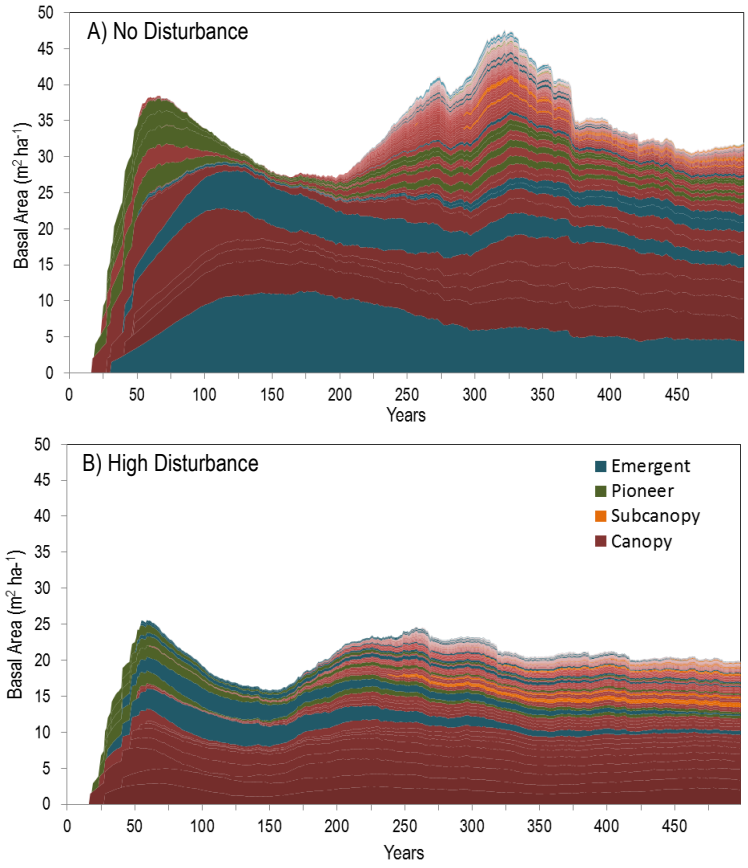

Fig. 2. (A) Model simulated successional development for all species modeled in ZELIG-TROP for a Central Amazon forest, separated by canopy growth form (emergent, canopy, sub-canopy, or pioneers). Species composition reported in individual basal area (m^2 ha^{-1}). **(B)** Model simulated successional development for all species modeled in ZELIG-TROP after the high-disturbance treatment.

1133

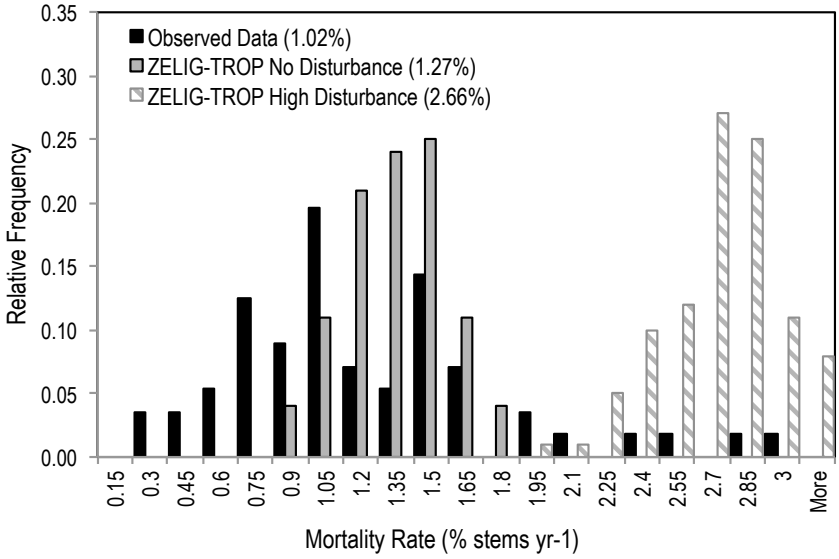

1134

1135 **Fig. 3**. Comparison of relative frequency of annual mortality rates (% stems year^{-1}) from observed

1136 data, ZELIG-TROP no-disturbance, and ZELIG-TROP high-disturbance model data after the

1137 disturbance treatment. (Observed data: Chambers et al. 2004).

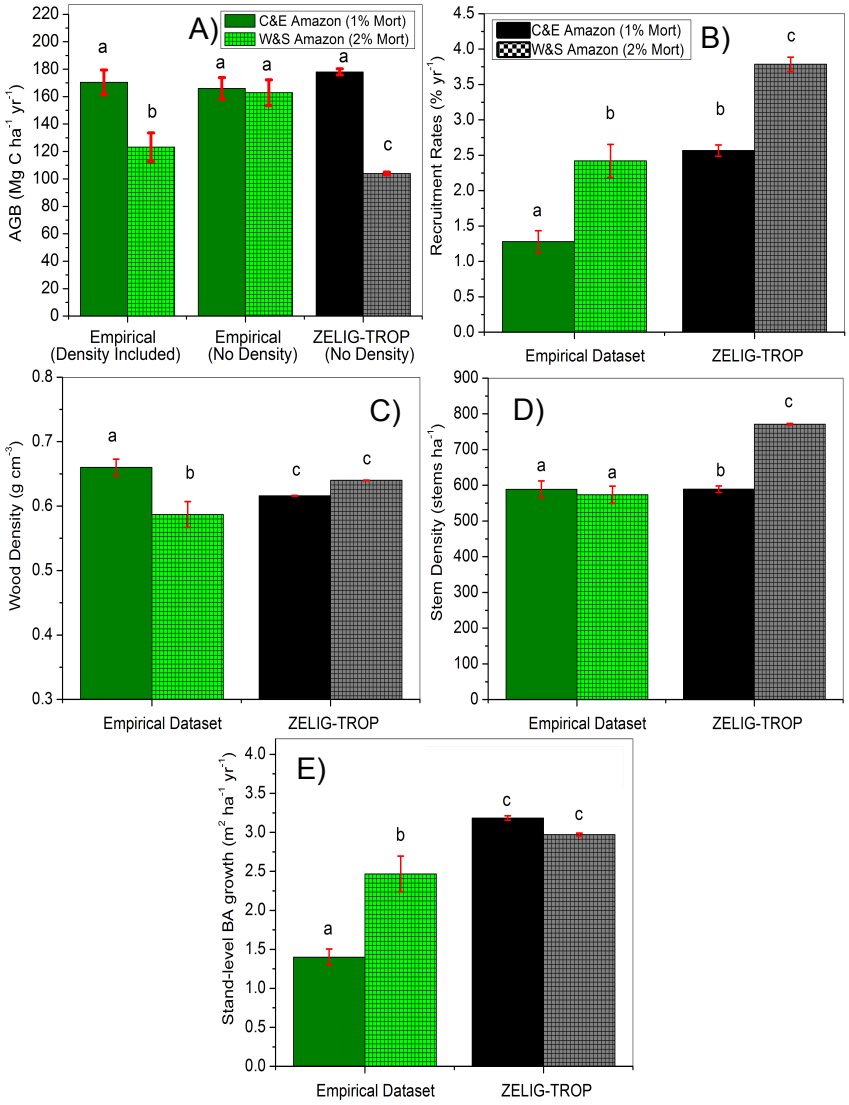

Fig. 4. Comparison between 'central and east' Amazon ("slow dynamics") and 'west and south' Amazon ("fast dynamics") between the empirical (RAINFOR dataset, green columns) and modeled ZELIG-TROP results for average **(A)** above-ground biomass (AGB, Mg C ha^{-1} yr^{-1}) with the observed dataset either including or not including wood density in the Chambers et al. (2001) allometric equation, **(B)** recruitment rate (% yr^{-1}), **(C)** average wood density (g cm^{-3}), **(D)** stem density (stems ha^{-1}), and **(E)** stand-level basal area (BA) growth rate (m^2 ha^{-1} yr^{-1}), with 95% CIs bars included. Different lower case letters represent significantly different values using Tukey's multiple comparison, following a one-way ANOVA.

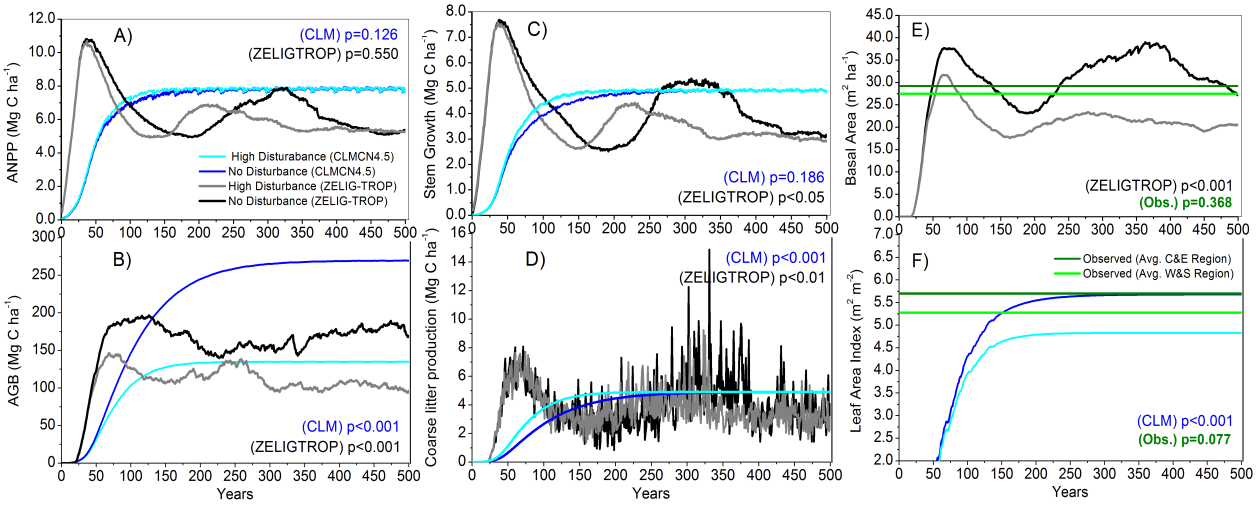

Fig. 5. CLM-CN model evaluation and comparisons to ZELIG-TROP for a no-disturbance scenario and a high disturbance treatment: **(A)** ANPP, **(B)** above-ground biomass, **(C)** stem growth, **(D)** coarse litter production rates, all measured in Mg C ha^{-1}, and **(E)** basal area from ZELIG-TROP and observed data in green as reported by Baker et al. (2004a), and **(F)** leaf area index (LAI) from CLM-CN4.5 and observed data in green as reported by McWilliams et al. (1993) and Malhi et al. (2013). Statistical significance test in all panels are two-sample Student's t-test between the no-disturbance and high disturbance treatments, separately for each model.

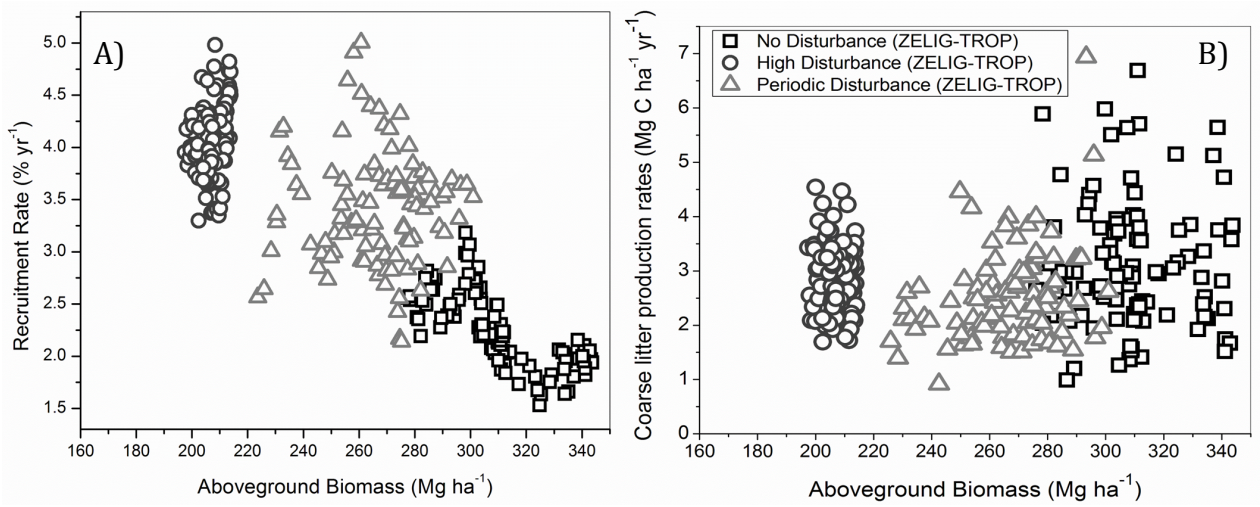

Fig. 6. **(A)** Relationship between above-ground biomass (Mg ha^{-1}) and recruitment rates (% yr^{-1}). **(B)** Relationship between above-ground biomass (Mg ha^{-1}) and coarse litter production rates as a result of tree mortality (Mg C ha^{-1} yr^{-1}), during a no-disturbance, high disturbance, and periodic disturbance simulation in ZELIG-TROP for the last 100 years of simulation.

1161

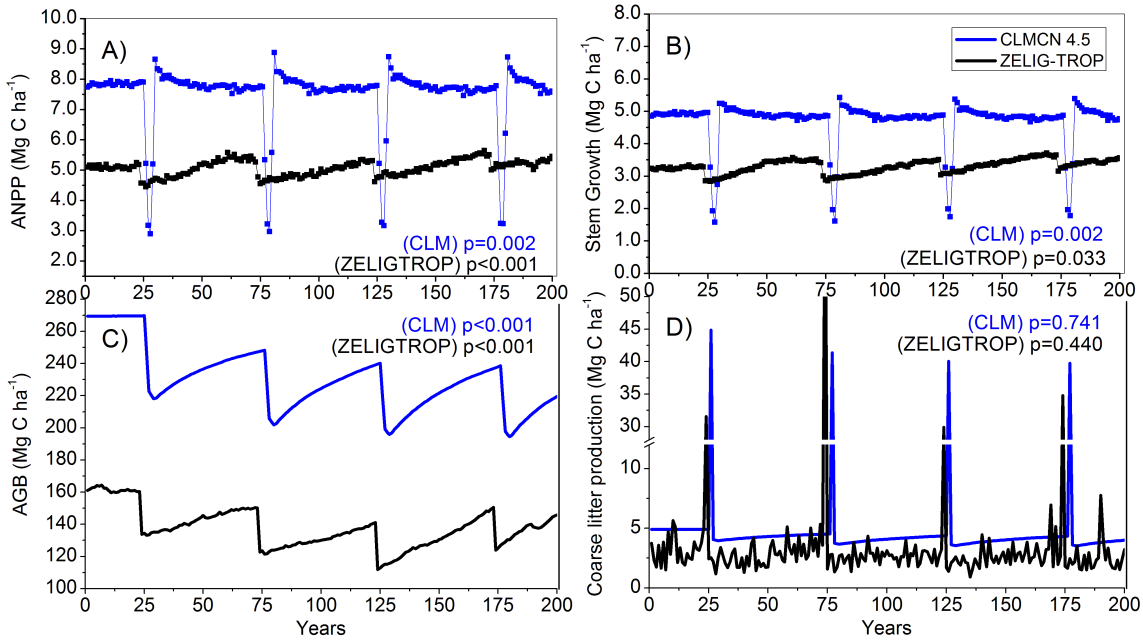

1162

1163 **Fig. 7**. CLM-CN model evaluation and comparisons to ZELIG-TROP for a periodic disturbance

1164 treatment: **(A)** ANPP, **(B)** stem growth, **(C)** aboveground biomass (AGB), and **(D)** coarse litter

1165 production rates, all measured in Mg C ha^{-1}. Statistical significance test in all panels are two-

1166 sample Student's t-test between the no-disturbance and high disturbance treatments, separately for

1167 each model.

Supplemental Material

Description of the Community Land Model (CLM):

The Community Land Model (CLM) is the land component of the Community Earth System Model (CESM) (Collins et al., 2006; Gent et al., 2011) that models global climate systems and makes projections of future climate change. In this study we used the stand-alone version of CLM4.5. This version used a data atmosphere model, a "stub" ocean, a stub sea-ice model, and the CLM-CN (carbon-nitrogen) version 4.5. Detailed descriptions of updates to version 4.0, algorithms used, and the general structure of CLM can be found in the CLM4.0 Technical Description (www.cesm.ucar.edu/models/cesm1.0/clm/CLM4_Tech_Note; Oleson et al., 2010; and Lawrence et al., 2011). This CN model included a prognostic carbon and nitrogen cycle in vegetation, litter, and soil organic matter (description in Thornton et al., 2007). For model comparisons against the gap model ZELIG-TROP, and observed field data, we used CLM results from a single grid point located at 2°35'S, 60°W, close to exact coordinate as the Central Amazon field transects. (Additional definitions of terms and parameters used in CLM are defined below).

In CLM, disturbance rates and realistically calculated plant mortality rates are ill represented. Currently, CLM includes two independent mechanisms for plant mortality: fire and natural senescence. In this study, mortality caused by fire was turned off. Mortality rates (representing natural senescence) are calculated as a whole-plant mortality that is intended to represent death of plants from all causes other than fire. This annual whole-plant mortality is calculated by removing 2% yr^{-1} of global total vegetation mass, regardless of differences in plant age, size, regional location, distribution of individuals, competition, or plant functional types (PFTs) (Oleson et al., 2010). We believe CLM could benefit from a more mechanistic approach of calculating plant mortality and disturbance. Developing a platform for CLM and CESM to

model tropical disturbance in a dynamic approach greatly enhances our understanding of future changes to carbon fluxes and atmospheric carbon dioxide levels. Another benefit of this new development to CESM is the capability to address disturbance within the newly coupled Integrated Earth System Model (iESM) (Jones et al., 2013; description available at http://climatemodeling.science.energy.gov/sites/default/files/iESM_Fact_Sheet.pdf). The iESM model combines the natural-human system with the biophysical and climate system by coupling three models: (1) CESM with the (2) Global Change Assessment Model (GCAM), which focuses on an energy/economic framework, and the (3) Global Land-Use Model (GLM). Therefore, the iESM project creates the capabilities to test the carbon market and energy market response to changes in forest mortality and increased disturbances.

Definition of the mortality algorithm in ZELIG-TROP and terms in each model

Plant mortality is determined in ZELIG-TROP by three separate means: age-related natural death, stress-related death, and external disturbance (evaluation of gap model mortality described in more detail in Keane et al. 2001). Natural mortality, or intrinsic death, is a tree level event that is stochastically determined, based on the assumptions that 1% of trees reach their maximum age, and that mortality was constant with respect to age (Botkin et al., 1972; Shugart, 1984). Stress related death, or growth-dependent mortality, is also a stochastic event in which death occurred to individuals that have a slow growth rate for two years or more due to suppression or environmental stressors. The model assumes that 1% of stressed individuals will live for 10 years (Shugart, 1984; Van Daalen and Shugart, 1989).

Within ZELIG-TROP the production of new organic matter from interval t_1 to t_2 is prognostically determined and given by: growth = $M_{t2} - M_{t1}$, where M_t is woody mass at time t. Growth is a

component needed to measure ANPP given by: ANPP = $M_{t2} - M_{t1} + L$, where L is both old and new litter loss. The annual loss of coarse woody material is given by: coarse litter production rate = $W_{L1} + W_{L2} + W_{L3}$, where W_{L1} are losses from natural death, W_{L2} are losses from stress related death, and W_{L3} are losses from disturbance (all trunks and branches >10cm in diameter). All flux values given in Mg C ha^{-1} yr^{-1}.

Within CLM the production of new organic matter from interval t_1 to t_2, is also prognostic, responding to environmental differences and in this study was estimated using the wood carbon allocation variable: woodc_alloc, which is given by: $growth_{CLM}$ = carbon to liveStem + carbon to deadStem + liveStem to storage + deadStem to storage. In CLM, ANPP (leaf, live stem, and dead stem) is given by: $ANPP_{CLM}$ = GPP – AR where AR is autotrophic respiration and is the sum of maintenance and growth respiration. Lastly, the annual loss of coarse woody material was estimated by the wood loss variable: woodc_loss, which is given by: coarse litter production $rate_{CLM}$ = liveStem to litter + deadStem to litter. All flux values given in Mg C ha^{-1} yr^{-1}.